ARTICLE

Distinct integrin activation pathways for effector and regulatory T cell trafficking and function

Hao Sun[1], Frederic Lagarrigue[1,2], Hsin Wang[1], Zhichao Fan[3], Miguel Alejandro Lopez-Ramirez[1], John T. Chang[1], and Mark H. Ginsberg[1]

Integrin activation mediates lymphocyte trafficking and immune functions. Conventional T cell (Tconv cell) integrin activation requires Rap1-interacting adaptor molecule (RIAM). Here, we report that *Apbb1ip⁻/⁻* (RIAM-null) mice are protected from spontaneous colitis due to IL-10 deficiency, a model of inflammatory bowel disease (IBD). Protection is ascribable to reduced accumulation and homing of Tconv cells in gut-associated lymphoid tissue (GALT). Surprisingly, there are abundant RIAM-null regulatory T cells (T reg cells) in the GALT. RIAM-null T reg cells exhibit normal homing to GALT and lymph nodes due to preserved activation of integrins αLβ2, α4β1, and α4β7. Similar to Tconv cells, T reg cell integrin activation and immune function require Rap1; however, lamellipodin (*Raph1*), a RIAM paralogue, compensates for RIAM deficiency. Thus, in contrast to Tconv cells, RIAM is dispensable for T reg cell integrin activation and suppressive function. In consequence, inhibition of RIAM can inhibit spontaneous Tconv cell–mediated autoimmune colitis while preserving T reg cell trafficking and function.

Introduction

The recruitment of leukocytes from the circulation to the gut mucosa plays a critical role in inflammatory bowel disease (IBD; Abraham and Cho, 2009; Adams and Eksteen, 2006; Braus and Elliott, 2009; Economou and Pappas, 2008; Eksteen et al., 2008; Kaser et al., 2010; Khor et al., 2011; Villablanca et al., 2011). Aberrant infiltration of mononuclear phagocytes, neutrophils, and inflammatory lymphocytes is observed in the colonic lamina propria of IBD patients (Caradonna et al., 2000; Smith et al., 2005). Adhesion molecules that mediate gut homing of leukocytes, such as integrin α4β7, have emerged as targets for IBD therapy (Berlin et al., 1995; Cominelli, 2013; Cox et al., 2010).

Leukocyte trafficking to gut and gut-associated lymphoid tissue (GALT) is precisely governed by integrins binding to their ligands, involving integrin αLβ2/intercellular adhesion molecule-1 (ICAM-1), α4β1/vascular cell adhesion molecule-1 (VCAM-1), and α4β7/mucosal addressin cell adhesion molecule-1 (MAdCAM-1; Noursharg et al., 2010; Sun et al., 2014). Integrin α4β7 is a proven therapeutic target in treating IBD (Feagan et al., 2013; Sandborn et al., 2013), but agents that completely block its functions are limited by potential redundancies with other integrins or by side effects (Feagan et al., 2013; Rutgeerts et al., 2013; Sun et al., 2020b). Indeed, in the murine IL-10–deficient spontaneous IBD model, genetic abrogation or antibody blockade of α4β7-mediated homing exacerbated colitis (Sun et al., 2020b). We ascribed this exacerbation to the inhibition of homing of

regulatory T cells (T reg cells) to GALT, because T reg cells play an essential role in suppressing intestinal inflammation (Rubtsov et al., 2008) and may therefore serve to limit IBD (Desreumaux et al., 2012; Li et al., 2010; Maul et al., 2005; Neurath, 2014; Wong et al., 2016).

Homing of lymphocytes to GALT requires integrin activation (Sun et al., 2018), a process whereby talin binding to the integrin β cytoplasmic domain causes a marked increase in the integrin's affinity (Kim et al., 2011). The binding of talin is regulated by the activation of Rap1, leading to its association with talin via the Rap1-interacting adaptor molecule (RIAM) adaptor (Han et al., 2006; Lagarrigue et al., 2015; Lee et al., 2009). This ternary Rap1–RIAM–talin complex can then associate with integrins in the T cell plasma membrane to mediate integrin activation and resulting homing and the formation of immunological synapses (Lagarrigue et al., 2017; Su et al., 2015). Thus, blockade of RIAM could suppress T cell–mediated autoimmune diseases, an idea supported by the reduction in diabetes induced by adoptive transfer of RIAM-null OT1 T cells (Lagarrigue et al., 2017). However, little is known about the role of RIAM in a spontaneous autoimmune disease. This question is of particular interest in the IL-10–deficient IBD model given the dramatic exacerbation of this model by blockade of integrin α4β7 functions (Sun et al., 2020a; Sun et al., 2020b).

[1]Department of Medicine, University of California, San Diego, La Jolla, CA; [2]Institut de Pharmacologie et Biologie Structurale, Université de Toulouse, Centre National de la Recherche Scientifique, Université Paul Sabatier, Toulouse, France; [3]Department of Immunology, School of Medicine, UConn Health, Farmington, CT.

Correspondence to Mark H. Ginsberg: mhginsberg@ucsd.edu.

Check for updates

Here, we show, in sharp contrast to the exacerbation of IL-10–deficient colitis by loss of integrin α4β7 function, genetic deletion of RIAM dramatically improves the colitis in this spontaneous autoimmune disease. The amelioration of colitis is due to reduced homing of RIAM-null Tconv cells to GALT. Surprisingly, although Rap1 is required for T reg cell function and RIAM is expressed in T reg cells, RIAM is dispensable for T reg cell homing to GALT. Furthermore, T reg cell function requires intact integrin activation (Klann et al., 2018); however, RIAM-null T reg cells exhibit intact activation of integrins α4β1, α4β7, and αLβ2 and normal suppressive function. Increased expression of lamellipodin (Lpd), a RIAM paralogue, accounts for the lack of RIAM requirement in T reg cells. These data demonstrate that T reg cells have a integrin activation pathway distinct from Tconv cells and identify RIAM as a focus for approaches to suppress the homing and function of Tconv cell cells while sparing T reg cells, thereby shifting the immunological balance in IBD and potentially other autoimmune disorders.

Results

RIAM deficiency protects IL-10–null mice from spontaneous colitis

To investigate the role of RIAM in the development of spontaneous autoimmune disease, we used the IL-10–deficient mouse strain (B6.129P2-$Il10^{tm1Cgn}$/J) that develops chronic colitis resembling IBD in humans (Kühn et al., 1993; Zhang et al., 2014b). IL-10–deficient mice were crossed with RIAM ($Apbb1ip$)–deficient mice, and the phenotypes of $Apbb1ip^{-/-}Il10^{-/-}$ and $Apbb1ip^{+/+}Il10^{-/-}$ mice were compared (Fig. 1).

As expected, $Apbb1ip^{+/+}Il10^{-/-}$ mice spontaneously developed diarrhea beginning at the age of 40–50 d under specific pathogen-free conditions. Chronic colitis became more evident in older $Apbb1ip^{+/+}Il10^{-/-}$ mice, as evidenced by diarrhea and bleeding (Fig. 1, D and E), with a significant loss of body weight (Fig. 1 A). More than 95% of these mice subsequently developed rectal prolapse (Fig. 1 B), and half of them died by 100 d of age (Fig. 1 C). In contrast, only approximately one quarter of the $Apbb1ip^{-/-}Il10^{-/-}$ mice developed rectal prolapse (Fig. 1 B), and their body weight increased at the same rate as $Il10^{+/+}$ mice (Fig. 1 A); strikingly, only 1 out of 23 $Apbb1ip^{-/-}Il10^{-/-}$ mice died by 100 d (Fig. 1 C). Histologically, IL-10 deficiency led to a severe colitis in $Apbb1ip^{+/+}$ mice, with almost complete loss of crypts, dense infiltrates of leukocytes in both mucosa and submucosa, and thickening of the bowel wall (Fig. 1 E). By contrast, the infiltrates in the $Apbb1ip^{-/-}Il10^{-/-}$ mice were much less prominent, and less tissue damage was observed (Fig. 1 E). Blinded histological scoring for inflammatory cell infiltrates and epithelial damage confirmed a reduction in the severity of colitis in $Apbb1ip^{-/-}Il10^{-/-}$ mice compared with $Apbb1ip^{+/+}Il10^{-/-}$ controls (Fig. 1 F). Along with increased inflammatory cell infiltration in $Apbb1ip^{+/+}Il10^{-/-}$ mice, colonic expression of proinflammatory cytokines (IL-1β, TNF-α, IL-6, IFN-γ, and IL-17A) was significantly reduced in $Apbb1ip^{-/-}Il10^{-/-}$ mice (Fig. 1 G).

RIAM is dispensable for T reg cell, but not Tconv cell, recruitment to the colon

Since RIAM plays an important role in leukocyte migration (Su et al., 2015), we enumerated CD4+ T cells in the colonic lamina

propria from $Apbb1ip^{-/-}Il10^{-/-}$ and $Apbb1ip^{+/+}Il10^{-/-}$ mice. $Apbb1ip^{-/-}Il10^{-/-}$ mice exhibited a marked reduction of Tconv cells in colonic lamina propria relative to $Apbb1ip^{+/+}Il10^{-/-}$ mice; in sharp contrast, there was no reduction in colonic T reg cells in $Apbb1ip^{-/-}Il10^{-/-}$ mice (Fig. 2 A). Accordingly, T reg cells represented a markedly increased fraction of CD4+ colonic lamina propria T cells in $Apbb1ip^{-/-}Il10^{-/-}$ mice (Fig. 2 A). Moreover, the fraction of splenic T reg cells in CD4+ T cells was unaffected by the lack of RIAM (Fig. 2 B). These findings suggest that, in contrast to Tconv cells, RIAM is dispensable for the presence of T reg cells in the colon in IL-10–deficient mice.

We used adoptive transfer (Ostanin et al., 2009; Song-Zhao and Maloy, 2014) to assess whether the beneficial effects of loss of RIAM function on colitis in IL-10–deficient mice might be in part due to reduced Tconv cell function. CD4+CD25−CD45RB^high T cells (Tconv cells) from $Apbb1ip^{+/+}$ or $Apbb1ip^{-/-}$ mice were infused into $Rag1^{-/-}$ recipient mice. $Rag1^{-/-}$ mice injected with $Apbb1ip^{+/+}$ Tconv cells manifested a dramatic loss in body weight after 20–30 d, and half of the mice died by 90 d (Fig. 2, C and D). In contrast, $Rag1^{-/-}$ mice injected with $Apbb1ip^{-/-}$ Tconv cells maintained body weight, and all mice survived (Fig. 2, C and D). In addition, the expression of colonic IL-1β, TNF-α, IL-6, IFN-γ, and IL-17A were also increased in $Rag1^{-/-}$ mice injected with $Apbb1ip^{+/+}$, but not $Apbb1ip^{-/-}$, Tconv cells (Fig. 2 E).

We next tested the role of RIAM in CD4+ T cell migration using a competitive homing assay. Consistent with previous studies (Klapproth et al., 2015; Lagarrigue et al., 2017; Su et al., 2015), bulk RIAM-deficient CD4+ T cells showed reduced homing to mesenteric LN (MLNs), Peyer's patches (PPs), and peripheral LNs (PLNs; Fig. 2 F). Thus, defective migration of RIAM-deficient CD4+ Tconv cells to the colon can account for their failure to induce colitis in this adoptive T cell transfer model.

RIAM-deficient T reg cells prevent colitis

We next assessed the effect of RIAM deficiency on the ability of T reg cells to prevent intestinal inflammation in the adoptive T cell transfer model (Song-Zhao and Maloy, 2014). Coinjection of WT T reg cells ($Apbb1ip^{+/+}$) and Tconv cells into $Rag1^{-/-}$ recipient mice, as expected, prevented colitis, as judged by maintenance of body weight (Fig. 3 A) and prevention of death (Fig. 3 B). $Rag1^{-/-}$ mice coinjected with $Apbb1ip^{-/-}$ T reg cells and WT Tconv cells also appeared healthy and continued to gain weight, similarly to those coinjected with $Apbb1ip^{+/+}$ T reg cells (Fig. 3, A and B). At 90 d, the reduced disease activity in the mice receiving coadministered RIAM-deficient T reg cells was similar to that of those receiving WT T reg cells (Fig. 3 C). The equivalent protection provided by RIAM-deficient T reg cells was confirmed by the marked suppression of colonic proinflammatory cytokines (Fig. 3 D). Thus, the lack of RIAM in T reg cells does not reduce their capacity to prevent adoptive T cell transfer–induced colitis.

RIAM-deficient T reg cells traffic to GALT and suppress T cell proliferation

To further characterize the role of RIAM in T reg cell function, we crossed floxed RIAM mice with $Foxp3^{YFP-Cre}$ mice (Rubtsov et al., 2008) to generate $Apbb1ip^{fl/fl},Foxp3^{YFP-Cre}$ mice in which the
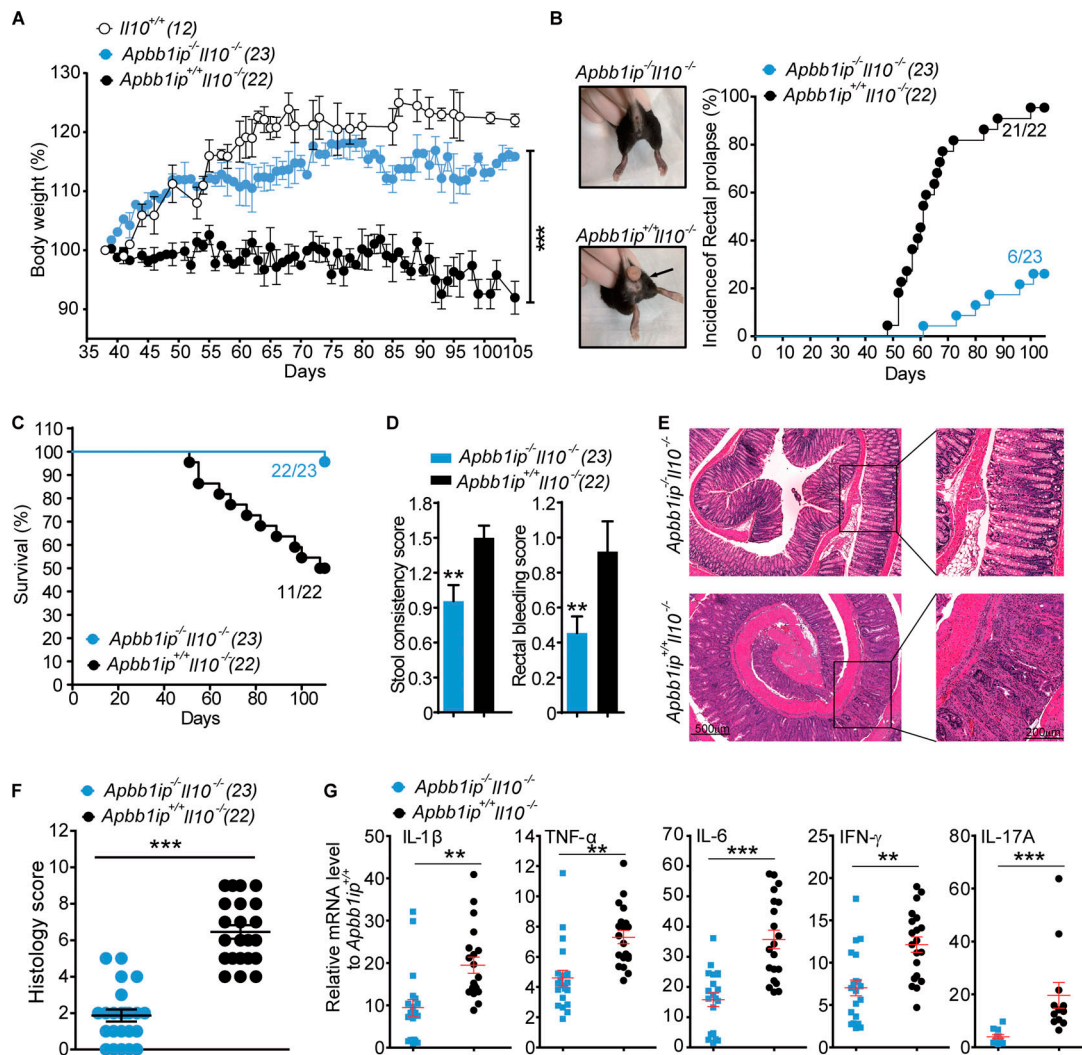
Figure 1. Loss of RIAM expression prevents IL-10 deficiency colitis. (A–D) Changes in body weight (A), rectal prolapsed occurrence (B), survival ratio (C), and stool consistency and rectal bleeding (D) of WT mice ($Il10^{+/+}$; $n = 12$), $Apbb1ip^{+/+}Il10^{-/-}$ mice ($n = 22$), and $Apbb1ip^{-/-}Il10^{-/-}$ mice ($n = 23$). Changes in body weight are shown as a percentage of the original weight. Stool consistency score: 0 (normal), 1 (soft), 2 (very soft), 3 (diarrhea); rectal bleeding score: 0 (none), 1 (red), 2 (dark red), 3 (gross bleeding). $n = 4$–6 mice per group. Data are representative of five independent experiments. Data represent mean ± SEM. Significant differences were determined using a two-way ANOVA with Bonferroni post test (A–C) or two-tailed t test (D). **(E and F)** Representative H&E staining of Swiss rolls of distal colon sections from $Apbb1ip^{+/+}Il10^{-/-}$ mice ($n = 23$) and $Apbb1ip^{-/-}Il10^{-/-}$ mice ($n = 22$) at day 100. Scale bars represent 500 μm or 200 μm. Histology score (F) as described in the Materials and methods section. $n = 4$–6 mice per group. Data are representative of five independent experiments. Data represent mean ± SEM. Significant differences were determined using a two-tailed t test. **(G)** mRNA expression of IL-1β, TNF-α, IL-6, IFN-γ, and IL-17A in distal colon tissue from $Apbb1ip^{-/-}Il10^{-/-}$ and $Apbb1ip^{+/+}Il10^{-/-}$ mice ($n = 12$–20). $n = 4$–6 mice per group. Data are representative of five (IL-1β, TNF-α, IL-6, and IFN-γ) or three (IL-17A) independent experiments. Results are normalized to GAPDH. Data represent mean ± SEM. Significant differences were determined using a two-tailed t test. **, $P < 0.01$; ***, $P < 0.001$. $Il10^{+/+}$, $Apbb1ip^{+/+}Il10^{+/+}$ mice.

gene encoding RIAM is specifically deleted in T reg cells ($Apbb1ip^{TRKO}$ mice). RIAM expression was undetectable in $Apbb1ip^{TRKO}$ T reg cells (Fig. 4 A) and can be used to trace T reg cells by the presence of YFP (YFP⁺; Fig. 4 A). $Apbb1ip^{TRKO}$ mice were born at expected frequencies and developed normally, with no overt signs of pathology in comparison with $Apbb1ip^{+/+}Foxp3^{YFP-Cre}$ littermates ($Apbb1ip^{+/+}$). Analysis of YFP⁺ T reg cells in MLNs, PPs, and PLNs showed no significant reduction in the abundance of T reg cells in comparison with $Apbb1ip^{+/+}$ littermates (Fig. S1 A). In agreement with previous studies (Klapproth et al., 2015; Lagarrigue et al., 2017; Su et al., 2015), deletion of RIAM in all T cells ($Apbb1ip^{CD4KO}$ mice) showed a dramatic decrease in T cell

numbers in LNs and PPs compared with $Apbb1ip^{+/+}CD4^{Cre}$ littermates ($Apbb1ip^{+/+}$; Fig. S1 B).

Talin plays a critical role in T reg cell–mediated maintenance of immune homeostasis (Klann et al., 2017). T reg cell–specific deletion of talin results in spontaneous lymphocyte activation associated with autoimmune failure to thrive resembling that observed in $Foxp3^{-/-}$ mice (Lahl et al., 2007) due to numerical and functional deficiencies of T reg cells in the periphery. Since RIAM plays a key role in talin-dependent Tconv cell integrin activation (Han et al., 2006), we investigated whether RIAM was also important for this T reg cell function. Examination of the resting (CD44^lo CD62L^hi) and previously activated (CD44^hi CD62L^lo) CD4⁺ and CD8⁺ T cell

Sun et al.
Integrin activation in T reg cells

Journal of Experimental Medicine   3 of 13
https://doi.org/10.1084/jem.20201524
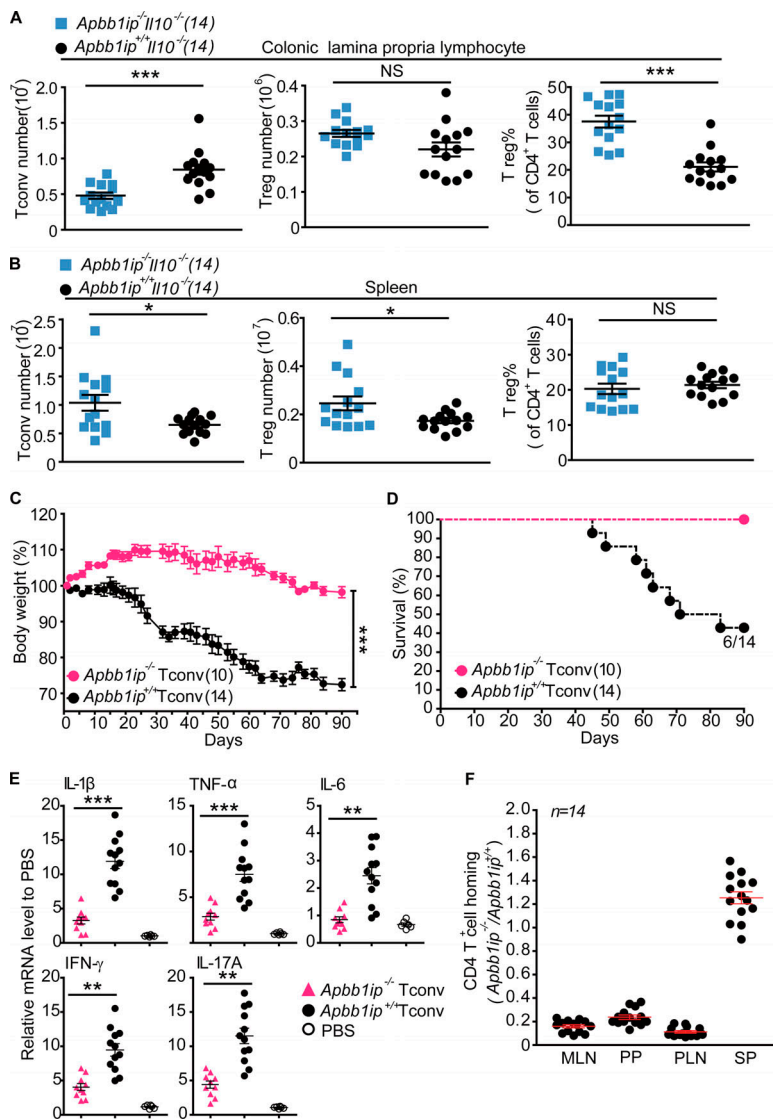
Figure 2. **Loss of RIAM expression has no effects on T reg cell recruitment to the colon but reduces the number of Tconv cells. (A and B)** Number and percentage of Tconv cells and T reg cells in colonic lamina propria lymphocyte (A) and SP (B) of $Apbb1ip^{+/+}Il10^{-/-}$ mice ($n = 14$) and $Apbb1ip^{-/-}Il10^{-/-}$ mice ($n = 14$). Cells were stained with CD4 and Foxp3. Tconv cell, CD4⁺Foxp3⁻; T reg cell, CD4⁺Foxp3⁺. $n = 4$–5 mice per group. Data are representative of three independent experiments. Data represent mean ± SEM. Significant differences were determined using a one-way ANOVA with Bonferroni posttest. *, $P < 0.05$; **, $P < 0.01$, ***, $P < 0.001$, $Apbb1ip^{-/-}$: $Apbb1ip^{-/-}Il10^{-/-}$ mice; $Apbb1ip^{+/+}$: $Apbb1ip^{+/+}Il10^{-/-}$ mice. **(C and D)** Adoptive transfer of $1 × 10^6$ CD4⁺CD25⁻CD45RB^high Tconv cells from $Apbb1ip^{+/+}$ or $Apbb1ip^{-/-}$ mice into $Rag1^{-/-}$ mice. **(C)** Changes in body weight. Data are shown as a percentage of the original weight. **(D)** Survival ratio. The number of mice in each group is indicated. $n = 3$–5 mice per group. Data are representative of three independent experiments. Data represent mean ± SEM. Significant differences were determined using a two-way ANOVA with Bonferroni posttest. **(E)** mRNA expression of IL-1β, TNF-α, IL-6, IFN-γ, and IL-17A in distal colon tissues from individual groups of mice in C and D. Results are normalized to GAPDH. $n = 3$–5 mice per group. Data are representative of three independent experiments. Data represent mean ± SEM. Significant differences were determined using a one-way ANOVA with Bonferroni posttest. **(F)** In vivo competitive homing of CD4⁺ T cells to different lymphoid tissues. CD4⁺ T cells were isolated from either $Apbb1ip^{+/+}$ or $Apbb1ip^{-/-}$ mice, differentially labeled, and mixed before injection into C57BL/6 mice. CD4⁺ T cells homed into different lymphoid organs were analyzed by flow cytometry 3 h after injection. The ratio of $Apbb1ip^{-/-}$ CD4⁺ T cells to $Apbb1ip^{+/+}$ CD4⁺ T cells from different lymphoid organs is shown ($n = 14$). $n = 3$–4 mice per group. Data are representative of four independent experiments. Data represent mean ± SEM. *, $P < 0.05$; **, $P < 0.01$; ***, $P < 0.001$. $Apbb1ip^{-/-}$ Tconv, mice injected with $Apbb1ip^{-/-}$ Tconv; $Apbb1ip^{+/+}$ Tconv, mice injected with $Apbb1ip^{+/+}$ Tconv.

compartments suggested that lack of T reg cell RIAM did not affect T lymphocyte activation in $Apbb1ip^{TRKO}$ mice (Fig. 4 B). We next assessed whether expression of RIAM was required for T reg cell suppressive functions. Using an in vitro suppression assay, we observed that T reg cells lacking RIAM were able to suppress Tconv cell proliferation (Fig. 4 C). Analysis of anti-inflammatory cytokines in RIAM-deficient T reg cells revealed no significant defect in the production of IL-10 or TGF-β1 (Fig. 4 D). We examined the role of RIAM in T reg cell migration using a competitive homing assay. Both WT and RIAM-deficient T reg cells homed equally well to MLNs, PPs, PLNs, and spleen (SP; Fig. 4 E). Taken together, these data show that RIAM is dispensable for T reg cell cytokine production, migration, and suppressive function.

RIAM is dispensable for T reg cell integrin activation

Leukocyte homing depends on integrin function (Hogg et al., 2011); in particular, T reg cell suppression is dependent on the integrin αLβ2–ICAM-1 interaction (Tran et al., 2009). RIAM is essential for activation of B and T cell integrins (Klapproth et al., 2015; Lagarrigue et al., 2017; Su et al., 2015), firm adhesion to

ICAM-1 and VCAM-1, and lymphocyte trafficking to secondary lymphoid organs. Because of the surprising preservation of both the suppressive function and homing of RIAM-null T reg cells, we assessed RIAM's importance for T reg cell integrin activation. Addition of PMA stimulated similar binding of soluble ICAM-1, VCAM-1, and MAdCAM-1 to both WT and RIAM-deficient T reg cells (Fig. 5 A), indicating that activation of integrins αLβ2, α4β1, and α4β7, respectively, was preserved in RIAM-deficient T reg cells. In sharp contrast, as expected (Lagarrigue et al., 2017; Su et al., 2015), RIAM-deficient CD4⁺ T cells showed a dramatic reduction in binding to ICAM-1 and MAdCAM-1 in both the resting state and after PMA stimulation (Fig. 5 B). In agreement with previous studies (Klapproth et al., 2015), binding to VCAM-1 was not affected in RIAM-null CD4⁺ T cells (Fig. 5 B). The surface expression of β1, β2, and β7 integrins in T reg cells or CD4⁺ T cells was not affected by the loss of RIAM (Fig. S2). In addition, we tested the static adhesion of T reg cells and CD4⁺ T cells on immobilized ICAM-1 or MAdCAM-1. Loss of RIAM expression resulted in defective adhesion of CD4⁺ T cells, whereas adhesion of T reg cells to both ICAM-1 and MAdCAM-1 was not
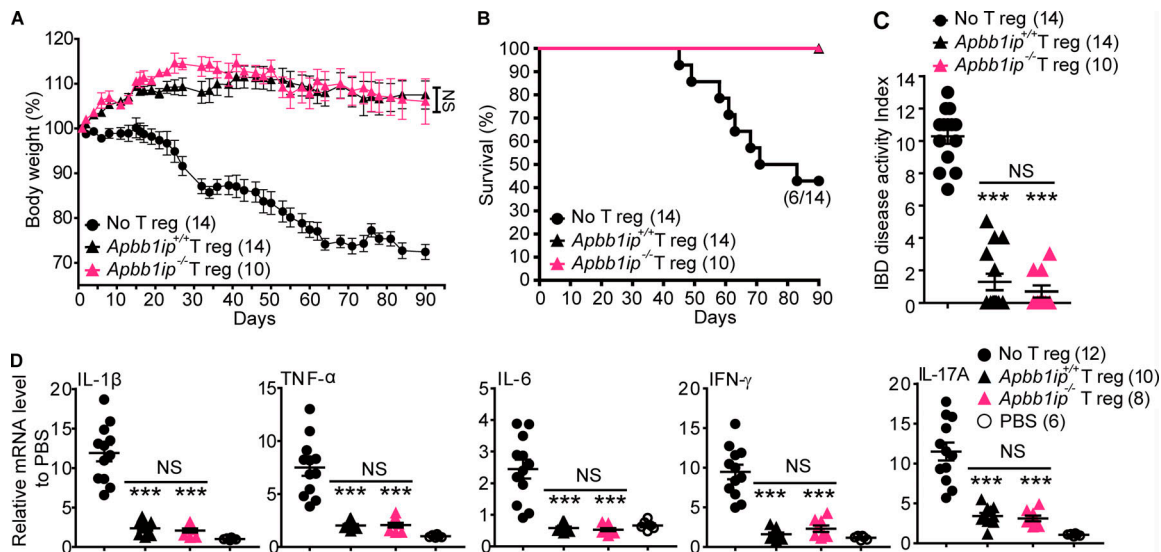
Figure 3. **RIAM-deficient T reg cells prevent adoptive T cell transfer–induced colitis.** 1×10^6 CD4+CD25−CD45RB^{high} Tconv cells isolated from WT C57BL/6 mice were injected into $Rag1^{-/-}$ mice in the presence or absence of 2×10^5 CD4+CD25+CD45RB^{low} T reg cells isolated from $Apbb1ip^{+/+}$ or $Apbb1ip^{-/-}$ mice. **(A and B)** Changes in body weight (A) and survival ratio (B) are shown. Changes in body weight are shown as a percentage of the original weight. The number of mice in each group is indicated. n = 3–5 mice per group. Data are representative of three independent experiments. Data represent mean ± SEM. Significant differences were determined using a two-way ANOVA with Bonferroni posttest. **(C)** IBD DAI. n = 3–5 mice per group. Data are representative of three independent experiments. Data represent mean ± SEM. Significant differences were determined using a one-way ANOVA with Bonferroni posttest. **(D)** RNA expression analysis of IL-1β, TNF-α, IL-6, IFN-γ, and IL-17A in distal colon tissue. Results are normalized to GAPDH. n = 2–4 mice per group. Data are representative of three independent experiments. Data represent mean ± SEM. Significant differences were determined using a one-way ANOVA with Bonferroni posttest. ***, $P < 0.001$. $Apbb1ip^{+/+}$ T reg, mice injected with WT Tconv cells; $Apbb1ip^{+/+}$ T reg; $Apbb1ip^{-/-}$ T reg, mice injected with WT Tconv cells and $Apbb1ip^{-/-}$ T reg cells; MFI, mean fluorescence intensity; No T reg, mice injected with WT Tconv cells. The $Apbb1ip^{+/+}$ T reg cell group and $Apbb1ip^{-/-}$ T reg cell group were compared with the "No T reg" group or each other in C and D.

impaired (Fig. 5, C and D). Thus, RIAM is dispensable for activation of multiple classes of integrin on T reg cells.

Talin and Rap1 are required for T reg cell function

Lymphocyte integrin activation is triggered by receptors such as chemokine, B cell, or T cell receptors (Abram and Lowell, 2009). A "canonical" pathway to lymphocyte integrin activation involves activation of Rap1 GTPase (Su et al., 2015); active Rap1 subsequently binds RIAM, which recruits cytoplasmic talin to the plasma membrane, where it binds to integrin β tails and triggers integrin activation (Han et al., 2006; Shattil et al., 2010). Because RIAM was dispensable for T reg cell integrin activation, we next examined the role of Rap1 in these cells.

We crossed $Rap1a^{fl/fl},Rap1b^{fl/fl}$ mice with $Foxp3^{YFP-Cre}$ mice to generate $Rap1a^{fl/fl},Rap1b^{fl/fl},Foxp3^{YFP-Cre}$ mice in which both Rap1a and Rap1b were deleted selectively in T reg cells ($Rap1a,b^{TRKO}$). Strikingly, male $Rap1a,b^{TRKO}$ mice developed systemic autoimmunity indicated by runting, dermatitis, lymphocytosis, and splenomegaly, ultimately resulting in death by 2–3 mo of age (Fig. S3, A–D), similar to T reg cell–specific talin1 knockout ($Tln1^{TRKO}$) mice or those expressing an integrin activation–defective talin1 (L325R; $Tln1^{L325R/TRKO}$; Klann et al., 2018). Rap1a,b-deficient T reg cells from either male or healthy female mice exhibited impaired binding to all three integrin ligands (Fig. 6 A). In the in vitro suppression assay, T reg cells lacking Rap1a,b did not suppress proliferation of Tconv cells (Fig. 6 E). In addition, these mice exhibited increased percentages of CD4+ T cells that displayed an activated (CD44^{hi}CD62L^{lo}) phenotype;

thus, Rap1a,b-deficient T reg cells result in inappropriate T cell activation in $Rap1a,b^{TRKO}$ mice (Fig. 6 B) associated with systemic autoimmunity. Taken together, these results indicate that unlike RIAM, Rap1 is indispensable for integrin activation in T reg cells.

Talin binding to the β integrin subunit is the final step in integrin activation (Kim et al., 2011), and, as shown above, $Rap1a,b^{TRKO}$ mice developed a profound defect in integrin activation. We therefore compared the effects of Rap1a and Rap1b deletion to talin1 deletion on T reg cell integrin activation. Rap1a,b-deficient T reg cells phenocopied the integrin activation defect in T reg cells from $Tln1^{TRKO}$ mice (Fig. 6 A). T cells from $Tln1^{TRKO}$ or $Rap1a,b^{TRKO}$ mice, which contain WT Tconv cells and Rap1a,b- or talin-deficient T reg cells, exhibited similar relative abundance of CD44^{hi}CD62^{lo} activated T cells (Fig. 6 B). We then adoptively transferred CD4+ T cells from $Tln1^{TRKO}$ or $Rap1a,b^{TRKO}$ mice into $Rag1^{-/-}$ mice. Both groups of mice showed a dramatic loss in body weight as early as 2–3 wk (Fig. 6 C), and half of both groups of mice died by 10 wk (Fig. 6 D) as a result of severe colitis. The suppressive activity of Rap1a,b- and talin1-null T reg cells was impaired to a similar degree (Fig. 6 E). Thus, Rap1a,b represents the principal upstream signaling pathway mediating talin-dependent integrin activation and functions in T reg cells.

Lpd compensates for the loss of RIAM in T reg cells function

RIAM is dispensable for T reg cell functions, leading us to ask whether another protein could serve as a bridge between Rap1 and talin1. Lpd is a RIAM paralogue that plays an important role in cell migration (Krause et al., 2004). We found Lpd was more
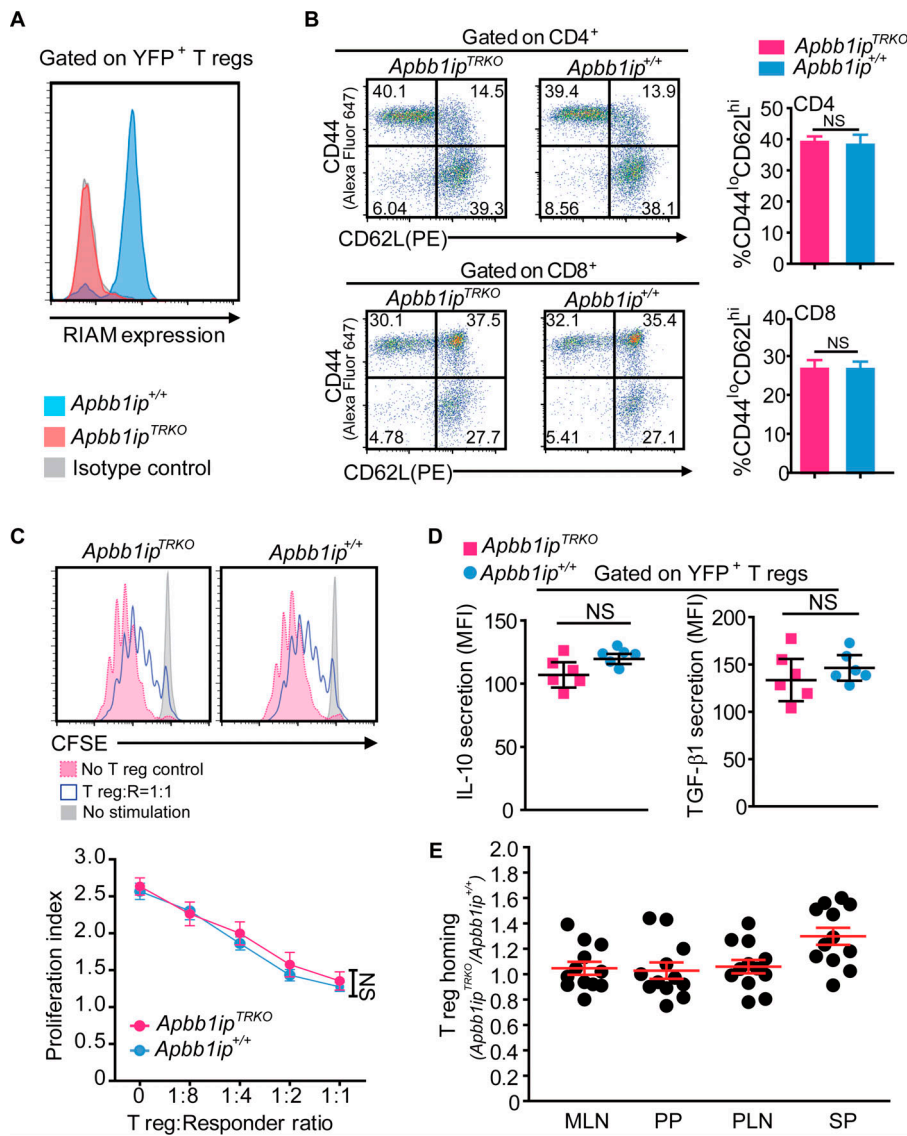
Figure 4. RIAM-deficient T reg cells exhibit intact suppressive activity and migration. (A) RIAM expression in T reg cells from $Apbb1ip^{+/+}$ or $Apbb1ip^{TRKO}$ mice. **(B)** Representative expression of CD44 and CD62L in splenic CD4+ (upper panels) and CD8+ (lower panels) T cells from $Apbb1ip^{+/+}$ and $Apbb1ip^{TRKO}$ mice. The percentage of CD44loCD62Lhi resting T cells is shown on the right. Data are representative of four independent experiments. Data represent mean ± SEM. Significant differences were determined using a two-tailed t test. **(C)** T reg cell suppressive activity. T reg cells isolated from CD45.2 congenic $Apbb1ip^{+/+}$ or $Apbb1ip^{TRKO}$ mice were mixed with responder cells at the indicated T reg cell/responder cell ratios. Responder cells are CFSE-labeled CD45.1 congenic C57BL/6 CD4+CD25− naive T cells activated by anti-CD3 (5 μg/ml), anti-CD28 (5 μg/ml), and IL-2. CFSE populations gated on CD45.1+ cells were analyzed by flow cytometry at 72 h to determine the proliferation index using FlowJo software. Data are representative of three independent experiments. Data represent mean ± SEM. Significant differences were determined using a two-way ANOVA with Bonferroni posttest. **(D)** Intracellular expression of IL-10 and TGFβ1 of GFP+ T reg cells from $Apbb1ip^{+/+}$ or $Apbb1ip^{TRKO}$ mice. Splenocytes were stimulated ex vivo with PMA and ionomycin in the presence of monensin (IL-10) or brefeldin A (TGFβ1) for 4 h at 37°C. Cells were fixed and permeabilized before staining ($n = 6$). Data are representative of three independent experiments. Data represent mean ± SEM. Significant differences were determined using a two-tailed t test. **(E)** In vivo competitive homing of T reg cells to different lymphoid tissues. YFP+ T reg cells were sorted from $Apbb1ip^{+/+}$ or $Apbb1ip^{TRKO}$ mice. Lymphoid organs were isolated 3 h after injection of T reg cells before flow cytometry analysis. The ratio of $Apbb1ip^{−/−}$ T reg cells (from $Apbb1ip^{TRKO}$ mice) to $Apbb1ip^{+/+}$ T reg cells (from $Apbb1ip^{+/+}$ mice) within various lymphoid tissues is shown ($n = 12$). $n = 4$ mice per group. Data are representative of three independent experiments. Data represent mean ± SEM. $Apbb1ip^{+/+}$, $Apbb1ip^{wt/wt},Foxp3^{YFP-Cre}$ mice; $Apbb1ip^{TRKO}$, $Apbb1ip^{fl/fl},Foxp3^{YFP-Cre}$ mice; TRKO, T reg cell–specific RIAM knockout.

highly expressed in T reg cells than in Tconv cells (Fig. 7 A). To explore the function of Lpd and RIAM, we crossed floxed Lpd mice or/and floxed RIAM mice with $Foxp3^{YFP-Cre}$ mice to specifically delete Lpd alone or in combination with RIAM in T reg cells ($Raph1^{TRKO}$ and $Raph1,Apbb1ip^{TRKO}$). Both $Raph1^{TRKO}$ and $Raph1,Apbb1ip^{TRKO}$ mice exhibited leukocytosis, with $Raph1,Apbb1ip^{TRKO}$ mice exhibiting even higher levels of neutrophils and lymphocytes in peripheral blood (Fig. S3 E). Lpd-deficient T reg cells exhibited reduction in their binding to ICAM-1 and MAdCAM-1, but not to VCAM-1. Lpd/RIAM-deficient T reg cells were even more profoundly affected, exhibiting an ~75% reduction in ICAM-1 and MAdCAM-1 binding and an ~40% decrease in VCAM-1 binding (Fig. 7 B). Thus, Lpd compensates for the loss of RIAM in T reg cell integrin activation, and Lpd and

RIAM are partially redundant. Consistent with the defect in integrin activation, the suppressive function of Lpd-deficient T reg cells was impaired and the suppressive function of Lpd/RIAM–deficient T reg cells reduced to an even greater extent (Fig. 7, C and D). In sharp contrast, deletion of Lpd in Tconv cells had a negligible effect on PMA-stimulated binding of soluble ICAM-1, VCAM-1, or MAdCAM-1, indicating that the activation of integrins αLβ2, α4β1, and α4β7 is preserved in Lpd-deficient CD4+ T cells (Fig. S4). As expected (Klapproth et al., 2015; Lagarrigue et al., 2017; Su et al., 2015), RIAM-deficient CD4+ T cells exhibited a profound reduction in their binding to ICAM-1 and MAdCAM-1, but not to VCAM-1. Taken together, these results show that both RIAM and Lpd are partially redundant for integrin activation and suppressive function in T
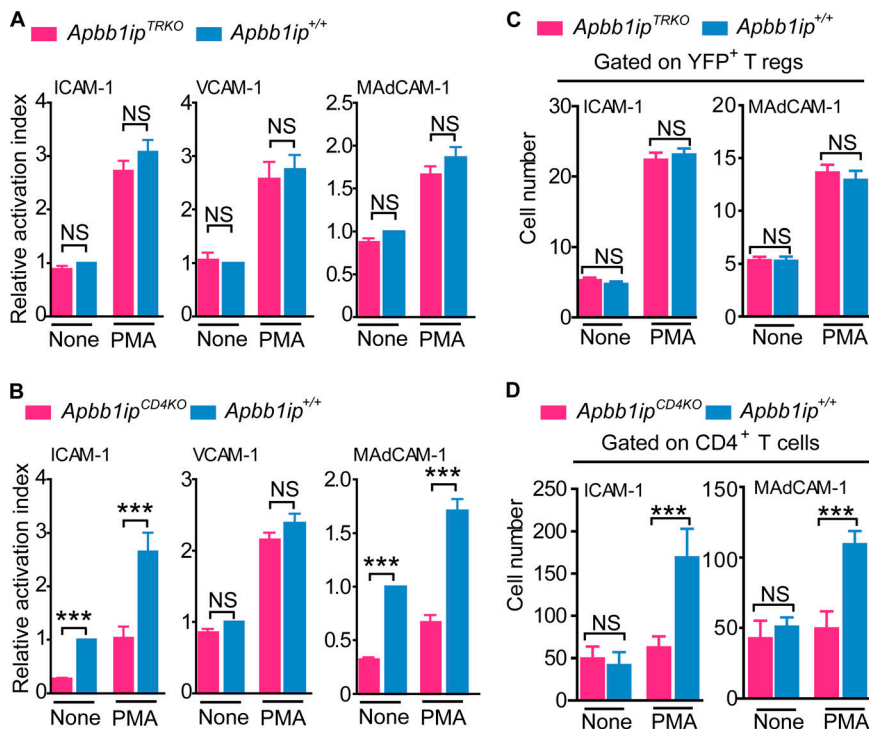
Figure 5. **RIAM-deficient T reg cells display intact integrin activation. (A and B)** Binding of soluble ICAM-1, VCAM-1, or MAdCAM-1 to YFP⁺ T reg cells isolated from *Apbb1ip⁺/⁺* (*Apbb1ipʷᵗ/ʷᵗ,Foxp3ʸᶠᴾ⁻ᶜʳᵉ*) or *Apbb1ipᵀᴿᴷᴼ* (*Apbb1ipᶠˡ/ᶠˡ,Foxp3ʸᶠᴾ⁻ᶜʳᵉ*) mice (A) or to CD4⁺ T cells isolated from *Apbb1ip⁺/⁺* (*Apbb1ipʷᵗ/ʷᵗ,CD4ᶜʳᵉ*) or *Apbb1ipᶜᴰ⁴ᴷᴼ* (*Apbb1ipᶠˡ/ᶠˡ,CD4ᶜʳᵉ*) mice (B) in the presence or absence of PMA (100 nM). **(C and D)** Static adhesion to ICAM-1 or MAdCAM-1 of YFP⁺ T reg cells isolated from *Apbb1ipᵀᴿᴷᴼ* mice (*Apbb1ip⁻/⁻*) or *Apbb1ipʷᵗ/ʷᵗ,Foxp3ʸᶠᴾ⁻ᶜʳᵉ* mice (*Apbb1ip⁺/⁺*; C), and CD4⁺ T cells isolated from *Apbb1ipᶜᴰ⁴ᴷᴼ* (*Apbb1ip⁻/⁻*) or *Apbb1ipʷᵗ/ʷᵗ,CD4ᶜʳᵉ* mice (*Apbb1ip⁺/⁺*; D). PMA concentration was 100 nM. Data are representative of five independent experiments. Data represent mean ± SEM. Significant differences were determined using a one-way ANOVA with Bonferroni posttest. ***, $P < 0.001$. *Apbb1ip⁺/⁺*: *Apbb1ipʷᵗ/ʷᵗ,Foxp3ʸᶠᴾ⁻ᶜʳᵉ* mice or *Apbb1ipʷᵗ/ʷᵗ,CD4ᶜʳᵉ* mice; *Apbb1ipᵀᴿᴷᴼ*, *Apbb1ipᶠˡ/ᶠˡ,Foxp3ʸᶠᴾ⁻ᶜʳᵉ* mice; CD4KO: CD4⁺ T cell–specific knockout; TRKO, T reg cell–specific RIAM knockout.

reg cells. Lpd makes a greater contribution to T reg cell integrin activation and consequently can compensate for loss of RIAM.

Discussion

RIAM is abundant in hematopoietic cells (Watanabe et al., 2008), and previous studies found that RIAM is essential for efficient leukocyte adhesion and proper trafficking of B and T cells to secondary lymphoid organs (Su et al., 2015), because RIAM mediates Rap1-dependent talin-induced integrin activation (Han et al., 2006; Lee et al., 2009). To investigate the role of RIAM in a spontaneous autoimmune disease, we used the IL-10–deficient mouse model (Kühn et al., 1993; Zhang et al., 2014b). This model is of particular interest because loss of integrin α4β7 function unexpectedly exacerbates IL-10 deficiency colitis due to impaired trafficking of T reg cells to GALT (Sun et al., 2020b). Here we report that, in contrast to inactivation of integrin β7, genetic inactivation of RIAM ameliorates spontaneous colitis in IL-10–deficient mice due to reduced trafficking of Tconv cells to GALT. Surprisingly, we found that there was increased relative abundance of T reg cells in the lamina propria of these IL-10–deficient mice. Furthermore, RIAM-deficient T reg cells exhibited normal homing to secondary lymphoid organs (including GALT), had normal suppressive function, and were able to inhibit development of colitis in an adoptive transfer model. Maintenance of these RIAM-deficient T reg cell functions was associated with preservation of activation of αLβ2, α4β7, and α4β1 integrins. As is true in other leukocytes, T reg cell integrin activation and function were dependent on talin (Yamahashi et al., 2015) and Rap1 GTPase (Su et al., 2015). Lpd, a RIAM paralogue, compensated for the lack of RIAM in T reg cell integrin activation and function. Thus, T reg cells use a distinct

integrin activation pathway from Tconv cells and other leukocytes. Earlier work had indicated that Tconv cells used ZAP-70 to proliferate but that T reg cell suppressive function is ZAP-70 independent (Au-Yeung et al., 2010); thus, there are other differences in regulatory pathways between T reg cells and Tconv cells. Inhibiting RIAM can suppress the trafficking and function of lymphocytes and neutrophils while sparing T reg cells, thereby shifting the immunological balance to ameliorate IBD and potentially other autoimmune and inflammatory diseases.

RIAM is dispensable for integrin activation in T reg cells and thus for T reg cells function. This was true for all three classes of leukocyte integrins (β1, β2, and β7), as assessed by agonist induced binding of ligands for αLβ2 (ICAM-1), α4β1 (VCAM-1), and α4β7 (MAdCAM-1). Integrin activation in response to chemokines was also preserved in RIAM-null T reg cells (Fig. S5). Lpd (Krause et al., 2004) is a member of the Mig-10/RIAM/Lpd family of adaptor proteins which contain an RA domain (Bailly, 2004) that can bind to Ras family GTPases, including Rap1. Although Lpd plays an important role in cell migration (Coló et al., 2012; Krause et al., 2004; Lagarrigue et al., 2015; Law et al., 2013), contains talin binding motifs (Lee et al., 2009), and can form a complex with integrins and talin (Lagarrigue et al., 2015), its role in Rap1-dependent integrin activation has been questioned (Zhang et al., 2014a). Here, we found the expression of Lpd is higher in T reg cells than Tconv cells and, consequently, that Lpd can compensate for the lack of RIAM in both integrin activation and T reg cell function (Figs. 6 and 7), thereby establishing the biological significance of Lpd in this critical regulator of the immune response. In the absence of Lpd, RIAM contributes to T reg cell function, because Lpd-RIAM double-deficient T reg cells exhibited a greater defect in T reg cell function, including impaired integrin activation and reduced
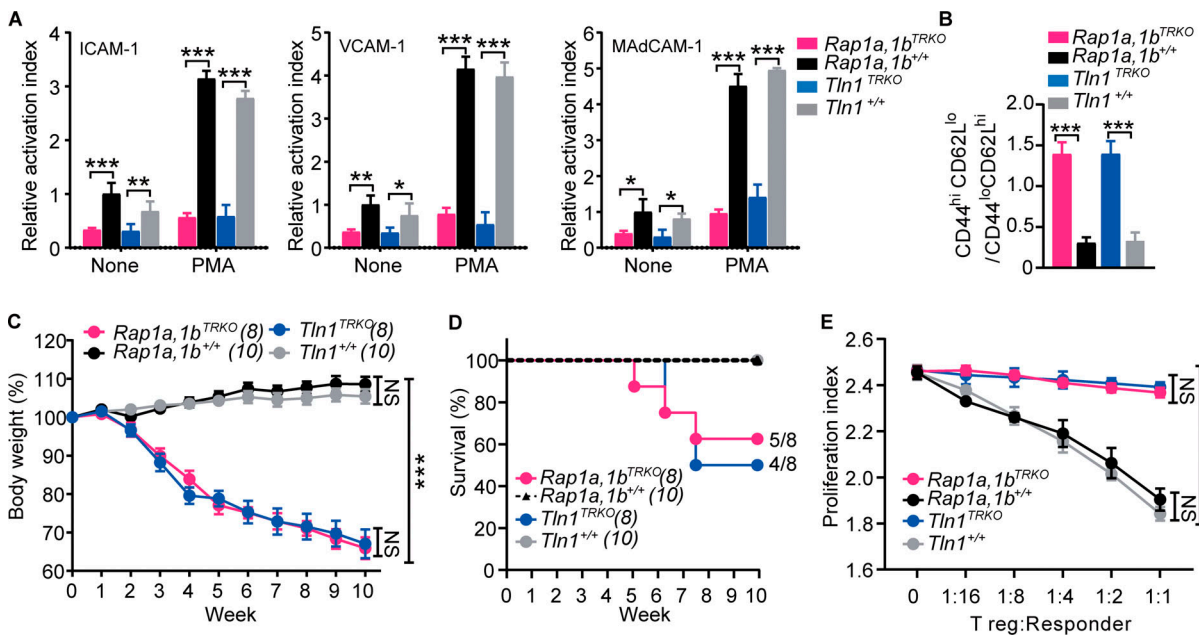
Figure 6. Loss of T reg cell Rap1a,b recapitulates the talin-null phenotype. (A) Binding of soluble ICAM-1, VCAM-1, or MAdCAM-1 to YFP$^+$ T reg cells isolated from *Rap1a,b$^{+/+}$*, *Rap1a,b^{TRKO}*, *TLN1$^{+/+}$*, or *TLN1^{TRKO}* mice in the presence or absence of PMA (100 nM). Data are representative of five independent experiments. Data represent mean ± SEM. Significant differences were determined using a one-way ANOVA with Bonferroni posttest. **(B)** Relative abundance of splenic CD4$^+$ T cells from *Rap1a,b$^{+/+}$* mice, *Rap1a,1b^{TRKO}* mice, *TLN1$^{+/+}$* mice, or *TLN1^{TRKO}* mice. The ratio of CD44^{hi}CD62L^{lo} T cells over CD44^{lo}CD62L^{hi} T cells is shown. Data are representative of three independent experiments. Data represent mean ± SEM. Significant differences were determined using a one-way ANOVA with Bonferroni posttest. **(C and D)** 2×10^6 CD4$^+$ T cells isolated from *Rap1a,b$^{+/+}$*, *Rap1a,1b^{TRKO}*, *TLN1$^{+/+}$*, or *TLN1^{TRKO}* mice were injected into *Rag1$^{-/-}$* mice to induce colitis. Changes in body weight (C) and survival ratio (D) are shown. The number of mice in each group is indicated. $n = 2–4$ mice per group. Data are representative of three independent experiments. Data represent mean ± SEM. Significant differences were determined using a two-way ANOVA with Bonferroni posttest. **(E)** T reg cell suppressive capability. T reg cells isolated from CD45.2 congenic *Rap1a,b$^{+/+}$*, *Rap1a,1b^{TRKO}*, *TLN1$^{+/+}$*, or *TLN1^{TRKO}* mice were mixed with responder cells at the indicated T reg cell/responder cell ratios. Responder cells are CFSE-labeled CD45.1 congenic C57BL/6 CD4$^+$CD25$^-$ naive T cells activated by anti-CD3 (5 μg/ml), anti-CD28 (5 μg/ml) and IL2. CFSE populations gated on CD45.1$^+$ cells were analyzed by flow cytometry at 72 h to determine the proliferation index using FlowJo software. Data are representative of three independent experiments. Data represent mean ± SEM. Significant differences were determined using a two-way ANOVA with Bonferroni posttest. *, $P < 0.05$; **, $P < 0.01$; ***, $P < 0.001$. *Rap1a,b$^{+/+}$*, *Rap1a$^{wt/wt}$,Rap1b$^{wt/wt}$,Foxp3$^{YFP-Cre}$* mice; *Rap1a,b^{TRKO}*, *Rap1a$^{fl/fl}$,Rap1b$^{fl/fl}$,Foxp3$^{YFP-Cre}$* mice; *TLN1$^{+/+}$*, *TLN1$^{wt/wt}$,Foxp3$^{YFP-Cre}$*; *TLN1^{TRKO}*, *TLN1$^{fl/fl}$,Foxp3$^{YFP-Cre}$* mice; *TRKO*, T reg cell–specific RIAM knockout.

suppressive capacity (Fig. 7 and Fig. S4 B). These results provide the first example of a biological role for Lpd in physiological integrin activation and show that Lpd can participate in this Rap1-dependent function.

Global loss of talin1, as well as combined loss of Rap1a and Rap1b, leads to embryonic lethality in mice (Calderwood et al., 2013; Li et al., 2007), whereas the RIAM-deficient mouse is viable and fertile without obvious developmental defects or abnormalities in platelet functions (Klapproth et al., 2015; Stritt et al., 2015; Su et al., 2015). RIAM plays a key role in talin-mediated activation of β2 integrins (Klapproth et al., 2015) in most leukocytes and therefore in their functions in immune responses and inflammation. We report here that RIAM is also crucial for β7 integrin activation in CD4$^+$ Tconv cells (Fig. 6). Blockade of leukocyte integrin function has long been appreciated to be a potential therapeutic approach in autoimmunity and inflammation (Dustin, 2019; von Andrian and Engelhardt, 2003). Indeed, the success of vedolizumab anti-α4β7 in IBD (Feagan et al., 2013), natalizumab anti-α4β1 in multiple sclerosis (Rice et al., 2005), and efalizumab anti-αLβ2 in psoriasis (Dedrick et al., 2002) all validate this principle. The latter two antibodies have encountered serious mechanism-based toxicities,

such as progressive multifocal leukoencephalopathy. In the case of integrin αIIbβ3, blockade of integrin activation can exert a therapeutic effect while reducing mechanism-based toxicities (Petrich et al., 2007a). Here, we show that the loss of Tconv cell integrin activation due to lack of RIAM can ameliorate a spontaneous model of IBD. Importantly, earlier studies had shown that loss of α4β7 integrin function in T reg cells can have a deleterious effect in IBD (Sun et al., 2020b; Zhang et al., 2016). In addition, we conclude that, in spite of RIAM's important role in Tconv cells, it is dispensable for T reg cell integrin activation and function; hence, RIAM inhibition is a candidate for fine tuning the immune response to inhibit effector T cells while sparing T reg cells.

Materials and methods
Antibodies and reagents
The following antibodies were from BioLegend: CD3 (17A2, 2C11), CD4 (GK1.5), CD8 (53–6.7), CD44 (1M7), CD62L (MEL-14), B220 (RA3-6B2), CD29 (HMβ1-1), CD18 (M18/2), β7 (FIB504), Foxp3 (MF-14), CD28 (37.51), IL-10 (JES5-16E3), and TGF-β1 (TW7-16B4). Secondary Alexa Fluor–labeled antibodies were
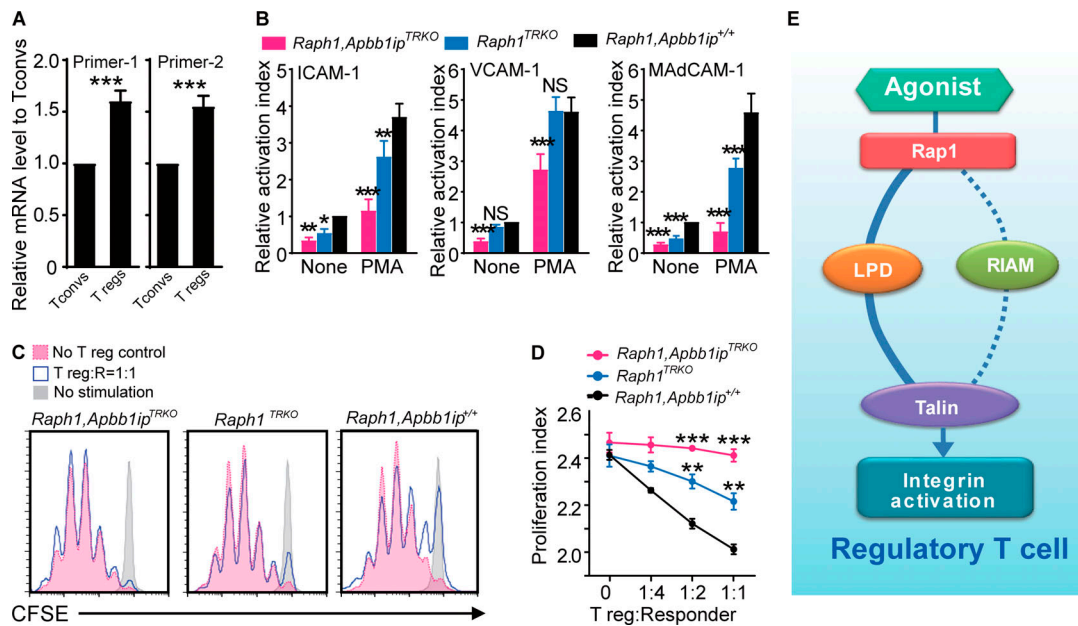
Figure 7. **Lpd plays an important role in T reg cell function. (A)** RNA expression of *Raph1* in Tconv cells and T reg cells. Results are normalized to GAPDH. Data are representative of three independent experiments. Data represent mean ± SEM. Significant differences were determined using a two-tailed *t* test. **(B)** Binding of soluble ICAM-1, VCAM-1, or MAdCAM-1 to YFP$^+$ T reg cells isolated from *Raph1,Apbb1ip$^{+/+}$*, *Raph1^{TRKO}*, or *Raph1,Apbb1ip^{TRKO}* mice in the presence or absence of PMA (100 nM). Data are representative of five independent experiments. Data represent mean ± SEM. Significant differences were determined using a one-way ANOVA with Bonferroni posttest. **(C and D)** T reg cell suppressive capability. T reg cells isolated from CD45.2 congenic *Raph1,Apbb1ip$^{+/+}$*, *Raph1^{TRKO}*, or *Raph1,Apbb1ip^{TRKO}* mice were mixed with responder cells at the indicated T reg cell/responder cell ratios. Responder cells are CFSE-labeled CD45.1 congenic C57BL/6 CD4$^+$CD25$^-$ naive T cells activated by anti-CD3 (5 μg/ml), anti-CD28 (5 μg/ml), and IL-2. CFSE populations gated on CD45.1$^+$ cells were analyzed by flow cytometry (C) at 72 h to determine the proliferation index using FlowJo software (D). Data are representative of three independent experiments. Data represent mean ± SEM. Significant differences were determined using a two-way ANOVA with Bonferroni posttest. **(E)** Integrin activation signaling pathway in T reg cells. In T reg cells, agonist stimulates Rap1 binding to Lpd and RIAM, leading talin binding to integrin β tail to activate integrins. *, P < 0.05; **, P < 0.01; ***, P < 0.001. *Raph1,Apbb1ip$^{+/+}$*, *Raph1$^{wt/wt}$,Apbb1ip$^{wt/wt}$,Foxp3$^{YFP-Cre}$* mice; *Raph1^{TRKO}*, *Raph1$^{fl/fl}$,Foxp3$^{YFP-Cre}$* mice; *Raph1,Apbb1ip^{TRKO}*, *Raph1$^{fl/fl}$,Apbb1ip$^{fl/fl}$,Foxp3$^{YFP-Cre}$* mice; TRKO, T reg cell–specific RIAM inactivation.

from Jackson ImmunoResearch. Foxp3 transcription factor fixation/permeabilization kit was purchased from eBioscience. CFSE and eFluor 670 were purchased from Invitrogen and BioLegend respectively. PMA and piroxicam were from Sigma. Ionomycin, brefeldin A, and monensin were from BioLegend. MojoSort mouse CD3 T cell isolation kit and mouse CD4 T cell isolation kit were from BioLegend. Liberase TL (Research Grade) and DNase I were from Roche. Recombinant mouse ICAM-1-Fc and VCAM-1-Fc were from R&D Systems. Recombinant mouse MAdCAM-1-Fc was purified by ProteinA beads as previously described (Sun et al., 2011).

Mice

All animal experiments were approved by the Institutional Animal Care and Use Committee of the University of California, San Diego, and conducted in accordance with federal regulations as well as institutional guidelines and regulations on animal studies. All mice were housed in specific pathogen–free conditions. C57BL/6 (CD45.1), C57BL/6 (CD45.2), *Il10$^{-/-}$*, and *Rag1$^{-/-}$* mice were from The Jackson Laboratory. *Apbb1ip$^{-/-}$*, *Apbb1ip$^{fl/fl}$*, *Tln1$^{fl/fl}$*, *Rap1a$^{fl/fl}$b$^{fl/fl}$*, *Rap1b$^{fl/fl}$*, *CD4^{Cre}*, *Foxp3$^{Cre-YFP}$*, and *Foxp3^{GFP}* mice have been described previously (Fontenot et al., 2005; Hogquist et al., 1994; Klapproth et al., 2015; Law et al., 2013; Lee et al., 2001; Petrich et al., 2007b; Rubtsov et al., 2008; Stefanini et al., 2014; Su et al., 2015). For experiments, 8–12-wk-old mice

were used. All injections of cells were performed during the light cycle. All experiments were performed by comparing mice with littermate controls, except for *Il10$^{-/-}$* background mice.

Mononuclear cells were isolated from MLNs, PPs, PLNs, SP, and colonic lamina propria as previously described (Berlin et al., 1995; Sun et al., 2014). Cell counting with immunofluorescence cytometry was performed using an Accuri C6 Plus and FACSCalibur (BD Biosciences).

Mouse colitis models

Il10$^{-/-}$ mice spontaneously develop a chronic IBD under specific pathogen–free conditions. The phenotypes of chronic colitis in *Il10$^{-/-}$* mice (C57BL/6 genetic background) became more evident at 10–12 wk. In a mixed C57BL/6-129/SvEv genetic background, the phenotypes of chronic colitis appeared earlier, at 6–8 wk. Because *Il10$^{-/-}$* mice develop spontaneous colitis, which has negative consequences on their capacity to breed, we separately crossed the mice as *Apbb1ip$^{+/+}$Il10$^{+/-}$* × *Apbb1ip$^{+/+}$Il10$^{+/-}$* and *Apbb1ip$^{-/-}$Il10$^{+/-}$* × *Apbb1ip$^{-/-}$Il10$^{+/-}$* to generate *Apbb1ip$^{+/+}$Il10$^{-/-}$* and *Apbb1ip$^{-/-}$Il10$^{-/-}$*, respectively. Sex-matched *Apbb1ip$^{+/+}$Il10$^{-/-}$* and *Apbb1ip$^{-/-}$Il10$^{-/-}$* mice were mixed together in a same cage starting at 3–4 wk. For piroxicam treatment, mice were administered piroxicam (200 ppm in diet, every day) for 2 wk and euthanized 3 wk after piroxicam treatment ended (Holgersen et al., 2014). For the adoptive T cell transfer model, 8–10-wk-old

mice were used. 5×10^5 CD4+CD25−CD45RB^{high} Tconv cells from C57BL/6 mice were injected intraperitoneally into $Rag1^{-/-}$ mice in the presence or absence of 1×10^5 CD4+CD25+CD45RB^{low} T reg cells derived from the indicated mice (0.2 ml PBS each recipient). Only comparison between littermates was considered.

Mouse body weight was measured daily, and values are shown as a percentage of the original weight. During the duration of the experiment, we assessed the clinical progression of colitis by daily blinded scoring a disease activity index (DAI) by two independent investigators. The DAI is the combined score of body weight loss, stool consistency, and rectal bleeding and prolapse as follows: (1) weight loss: 0 (no loss), 1 (1–5%), 2 (5–10%), 3 (10–20%), or 4 (>20%); (2) stool consistency: 0 (normal), 1 (soft), 2 (very soft), or 3 (diarrhea); (3) rectal bleeding: 0 (none), 1 (red), 2 (dark red), or 3 (gross bleeding); and (4) rectal prolapse: 0 (none), 1 (signs of prolapse), 2 (clear prolapse), or 3 (extensive prolapse). Mice were sacrificed at week 15.

Histology
Formalin-fixed, paraffin-embedded Swiss-rolled colon sections of 4-mm thickness were mounted on glass slides and followed by H&E staining or periodic acid–Schiff staining. Images were acquired with a Nanozoomer 2.0HT Slide Scanner (Hamamatsu). Blinded histological scoring was performed by two investigators based on the method described previously (Erben et al., 2014), and total scoring range is 0–12 (Table 1).

Flow cytometry
Cells isolated from mouse tissues were washed and resuspended in PBS containing 0.1% BSA and stained with conjugated antibody for 30 min at 4°C. Then, cells were washed twice before flow cytometry analysis using an Accuri C6 Plus or FACSCalibur (BD Biosciences). Data were analyzed using FlowJo software. For soluble ligand binding assay, 5×10^6 cells were washed and resuspended in HBSS containing 0.1% BSA and 1 mM Ca^{2+}/Mg^{2+} before incubation with integrin ligands for 30 min at 37°C in presence with or without 100 nM PMA. Cells were then incubated with Alexa Fluor 647–conjugated anti-human IgG (1:200) for 30 min at 4°C. For intracellular detection of cytokines, splenocytes were stimulated ex vivo with PMA and ionomycin in the presence of brefeldin A and monensin for 6 h at 37°C; cells were fixed in 4% paraformaldehyde (Electron Microscopy Services) and permeabilized with the Foxp3 transcription factor fixation/permeabilization kit (eBioscience) before IL-10, TGF-β1, and Foxp3 staining.

Static cell adhesion assay
Coverslips were coated with integrin ligand in coating buffer (PBS and 10 mM NaHCO$_3$, pH 9.0) overnight at 4°C. The coverslips were then rinsed with PBS and free binding sites were blocked with 2% BSA in coating buffer for 1 h at 37°C. Splenocytes were added onto coverslips, and adhesion was allowed for 1 h at 37°C. Coverslips were next washed with PBS and fixed with 2% paraformaldehyde at room temperature for 15 min. Bound cells were observed using a Keyence BZX-700 all-in-one fluorescence microscope with CFI Plan Apo λ4× fluorescent

Table 1. Scoring scheme used for the $Il10^{-/-}$ mouse model

Score	Description
Epithelium	
0	Normal
1	Hyperproliferation, irregular crypts, goblet cell loss
2	Mild to moderate crypt loss (10–50%)
3	Severe crypt loss (50–90%)
4	Complete crypt loss, surface epithelium intact
5	Small to medium-sized ulcer (<10 crypt widths)
6	Large ulcer (>10 crypt widths)
Infiltration with inflammatory cells	
Mucosa	
0	None
1	Mild infiltration
2	Moderate infiltration
3	Severe infiltration
Submucosa	
0	None
1	Mild to moderate infiltration and/or edema
2	Severe infiltration
Muscularis/serosa	
0	Not involved
1	Involved

Total scoring range: 0–12.

objective (Nikon Plan Apochromat, NA 0.2) or CFI Plan Apo λ10× fluorescent objective (Nikon Plan Apochromat, NA 0.45), which was operated with a 2/3-inch, 2.83-million-pixel monochrome charge-coupled device (colorized with LC filter) at 25°C.

T reg cell suppression assays
CD4+CD25− T cells (responder cells) were isolated from SPs of C57BL/6 (CD45.1) WT mice by magnetic separation using the CD4+ T cell–negative isolation kit (BioLegend); a biotin-conjugated anti-CD25 (PC61; BioLegend) antibody was included to deplete T reg cells. YFP+ T reg cells were sorted with a FACSAria 2 (BD Biosciences). Responder cells were labeled with CFSE and cocultured with T reg cells (8:1, 4:1, 2:1, and 1:1 ratios) in the presence of 5 μg/ml immobilized antibodies against CD3 (2C11) and CD28 (37.51) and $IL2$ for 4 d at 37°C. The proliferation index was calculated by FlowJo v10.

In vivo competitive lymphocyte homing
The competitive homing assay used high- and low-dose cell tracker as described previously (Haeryfar et al., 2008). YFP+ T reg cells were sorted with a FACSAria 2 (BD Biosciences) from $Apbb1ip^{+/+}$ and $Apbb1ip^{TRKO}$ mice and labeled with 1 μM and 10 μM eFluor670, respectively, resulting in readily discriminated cell populations. Equal numbers (1×10^7) of differentially labeled T reg cells were mixed and then intravenously injected

Sun et al.
Integrin activation in T reg cells

Journal of Experimental Medicine 10 of 13
https://doi.org/10.1084/jem.20201524

Table 2. **Sequences of primers used for real-time quantitative PCR analyses**

Primer	Direction	Sequence (5′–3′)
IL-1β	Forward	AGTGTGGATCCCAAGCAATAC
	Reverse	CTCCACTTTGCTCTTGACTTCT
TNF-α	Forward	AGTGACAAGCCTGTAGCCC
	Reverse	GAGGTTGACTTTCTCCTGGTAT
IL-6	Forward	CTGCAAGAGACTTCCATCCAGTT
	Reverse	GAAGTAGGGAAGGCCGTGG
IFN-γ	Forward	CTCTTCCTCATGGCTGTTTCT
	Reverse	TTCTTCCACATCTATGCCACTT
GAPDH	Forward	CCAGGTTGTCTCCTGCGACTT
	Reverse	CCTGTTGCTGTAGCCGTATTCA

into C57BL/6 recipient mice. Lymphoid organs were harvested 3 h after injection, and isolated cells were analyzed by flow cytometry. The ratio of *Apbb1ip*$^{−/−}$ T reg cells (eFluor670^{high}) to *Apbb1ip*$^{+/+}$ T reg cells (eFluor670^{low}) from different lymphoid organs is shown. For the competitive homing assay of RIAM-deficient CD4$^+$ T cells, CD4$^+$ T cells were isolated by MojoSort mouse CD4 T cell isolation kit (BioLegend) from *Apbb1ip*$^{+/+}$ or *Apbb1ip*^{CD4KO} mice and labeled with 1 μM CFSE and eFluor670, respectively.

Real-time quantitative PCR analyses
Total RNA was isolated from colon using tissue homogenizer (JXFSTPRP-24; ThunderSci) and TRIzol reagent according to the manufacturer's protocol (Thermo Fisher Scientific). For gene expression analysis, single-stranded cDNA was produced from 10 μg total RNA of colon using SuperScript III First-Strand synthesis and oligo-dT primers according to the manufacturer's protocol (Thermo Fisher Scientific). Kappa SybrFast qPCR kit (Kapa Biosystems) and thermal cycler (CFX96 Real-Time System; Bio-Rad) were used to determine the relative levels of the genes analyzed (primer sequences are shown in Table 2) according to the manufacturer's protocol. The 2$^{−ΔΔCT}$ method was used for analysis, and data were normalized to GAPDH. Control values (WT mice or *Rag*$^{−/−}$ mice injected with PBS) were set to 1 for comparisons.

Statistical analysis
Statistical analysis was performed using Prism software (version 8.00; GraphPad Software), and all datasets were checked for Gaussian normality distribution. Data analysis was performed using a two-tailed *t* test, one-way ANOVA, or two-way ANOVA followed by Bonferroni posttest as indicated in the figure legends. The resulting P values are indicated as follows: NS, P > 0.05; *, P < 0.05; **, P < 0.01; ***, P < 0.001. Plotted data show the mean ± SEM of three to five independent experiments.

Online supplemental material
Fig. S1 shows RIAM-deficient T reg cells have a similar number and percentage of T reg cells in lymphoid organs compared with WT T reg cells. Fig. S2 shows RIAM-deficient T cells or T reg cells have similar integrin expression levels compared with WT cells. Fig. S3 shows that mice with T reg cell–specific deletion of Rap1a,b have spontaneous lethal inflammation and shows blood cells counts in these T reg cell–specific gene–depleted mice. Fig. S4 shows the role of Lpd in Tconv cells. Fig. S5 shows integrin activation in response to chemokines in T reg cell–specific gene–depleted mice.

References
Abraham, C., and J.H. Cho. 2009. Inflammatory bowel disease. *N. Engl. J. Med.* 361:2066–2078. https://doi.org/10.1056/NEJMra0804647

Abram, C.L., and C.A. Lowell. 2009. The ins and outs of leukocyte integrin signaling. *Annu. Rev. Immunol.* 27:339–362. https://doi.org/10.1146/annurev.immunol.021908.132554

Adams, D.H., and B. Eksteen. 2006. Aberrant homing of mucosal T cells and extra-intestinal manifestations of inflammatory bowel disease. *Nat. Rev. Immunol.* 6:244–251. https://doi.org/10.1038/nri1784

Au-Yeung, B.B., S.E. Levin, C. Zhang, L.Y. Hsu, D.A. Cheng, N. Killeen, K.M. Shokat, and A. Weiss. 2010. A genetically selective inhibitor demonstrates a function for the kinase Zap70 in regulatory T cells independent of its catalytic activity. *Nat. Immunol.* 11:1085–1092. https://doi.org/10.1038/ni.1955

Bailly, M. 2004. Ena/VASP family: new partners, bigger enigma. *Dev. Cell.* 7:462–463. https://doi.org/10.1016/j.devcel.2004.09.008

Berlin, C., R.F. Bargatze, J.J. Campbell, U.H. von Andrian, M.C. Szabo, S.R. Hasslen, R.D. Nelson, E.L. Berg, S.L. Erlandsen, and E.C. Butcher. 1995. alpha 4 integrins mediate lymphocyte attachment and rolling under physiologic flow. *Cell.* 80:413–422. https://doi.org/10.1016/0092-8674(95)90491-3

Braus, N.A., and D.E. Elliott. 2009. Advances in the pathogenesis and treatment of IBD. *Clin. Immunol.* 132:1–9. https://doi.org/10.1016/j.clim.2009.02.006

Calderwood, D.A., I.D. Campbell, and D.R. Critchley. 2013. Talins and kindlins: partners in integrin-mediated adhesion. *Nat. Rev. Mol. Cell Biol.* 14:503–517. https://doi.org/10.1038/nrm3624

Caradonna, L., L. Amati, P. Lella, E. Jirillo, and D. Caccavo. 2000. Phagocytosis, killing, lymphocyte-mediated antibacterial activity, serum autoantibodies, and plasma endotoxins in inflammatory bowel disease. *Am. J. Gastroenterol.* 95:1495–1502. https://doi.org/10.1111/j.1572-0241.2000.02085.x

Coló, G.P., E.M. Lafuente, and J. Teixidó. 2012. The MRL proteins: adapting cell adhesion, migration and growth. *Eur. J. Cell Biol.* 91:861–868. https://doi.org/10.1016/j.ejcb.2012.03.001

Cominelli, F. 2013. Inhibition of leukocyte trafficking in inflammatory bowel disease. *N. Engl. J. Med.* 369:775–776. https://doi.org/10.1056/NEJMe1307415

Cox, D., M. Brennan, and N. Moran. 2010. Integrins as therapeutic targets: lessons and opportunities. *Nat. Rev. Drug Discov.* 9:804–820. https://doi.org/10.1038/nrd3266

Dedrick, R.L., P. Walicke, and M. Garovoy. 2002. Anti-adhesion antibodies efalizumab, a humanized anti-CD11a monoclonal antibody. *Transpl. Immunol.* 9:181–186. https://doi.org/10.1016/S0966-3274(02)00029-1

Desreumaux, P., A. Foussat, M. Allez, L. Beaugerie, X. Hébuterne, Y. Bouhnik, M. Nachury, V. Brun, H. Bastian, N. Belmonte, et al. 2012. Safety and efficacy of antigen-specific regulatory T-cell therapy for patients with refractory Crohn's disease. *Gastroenterology.* 143:1207–1217.e2. https://doi.org/10.1053/j.gastro.2012.07.116

Dustin, M.L. 2019. Integrins and Their Role in Immune Cell Adhesion. *Cell.* 177:499–501. https://doi.org/10.1016/j.cell.2019.03.038

Economou, M., and G. Pappas. 2008. New global map of Crohn's disease: Genetic, environmental, and socioeconomic correlations. *Inflamm. Bowel Dis.* 14:709–720. https://doi.org/10.1002/ibd.20352

Eksteen, B., E. Liaskou, and D.H. Adams. 2008. Lymphocyte homing and its role in the pathogenesis of IBD. *Inflamm. Bowel Dis.* 14:1298–1312. https://doi.org/10.1002/ibd.20453

Erben, U., C. Loddenkemper, K. Doerfel, S. Spieckermann, D. Haller, M.M. Heimesaat, M. Zeitz, B. Siegmund, and A.A. Kühl. 2014. A guide to histomorphological evaluation of intestinal inflammation in mouse models. *Int. J. Clin. Exp. Pathol.* 7:4557–4576.

Feagan, B.G., P. Rutgeerts, B.E. Sands, S. Hanauer, J.F. Colombel, W.J. Sandborn, G. Van Assche, J. Axler, H.J. Kim, S. Danese, et al. GEMINI 1 Study Group. 2013. Vedolizumab as induction and maintenance therapy for ulcerative colitis. *N. Engl. J. Med.* 369:699–710. https://doi.org/10.1056/NEJMoa1215734

Fontenot, J.D., J.L. Dooley, A.G. Farr, and A.Y. Rudensky. 2005. Developmental regulation of Foxp3 expression during ontogeny. *J. Exp. Med.* 202:901–906. https://doi.org/10.1084/jem.20050784

Haeryfar, S.M., H.D. Hickman, K.R. Irvine, D.C. Tscharke, J.R. Bennink, and J.W. Yewdell. 2008. Terminal deoxynucleotidyl transferase establishes and broadens antiviral CD8+ T cell immunodominance hierarchies. *J. Immunol.* 181:649–659. https://doi.org/10.4049/jimmunol.181.1.649

Han, J., C.J. Lim, N. Watanabe, A. Soriani, B. Ratnikov, D.A. Calderwood, W. Puzon-McLaughlin, E.M. Lafuente, V.A. Boussiotis, S.J. Shattil, and M.H. Ginsberg. 2006. Reconstructing and deconstructing agonist-induced activation of integrin alphaIIbbeta3. *Curr. Biol.* 16:1796–1806. https://doi.org/10.1016/j.cub.2006.08.035

Hogg, N., I. Patzak, and F. Willenbrock. 2011. The insider's guide to leukocyte integrin signalling and function. *Nat. Rev. Immunol.* 11:416–426. https://doi.org/10.1038/nri2986

Hogquist, K.A., S.C. Jameson, W.R. Heath, J.L. Howard, M.J. Bevan, and F.R. Carbone. 1994. T cell receptor antagonist peptides induce positive selection. *Cell.* 76:17–27. https://doi.org/10.1016/0092-8674(94)90169-4

Holgersen, K., P.H. Kvist, H. Markholst, A.K. Hansen, and T.L. Holm. 2014. Characterisation of enterocolitis in the piroxicam-accelerated interleukin-10 knock out mouse--a model mimicking inflammatory bowel disease. *J. Crohn's Colitis.* 8:147–160. https://doi.org/10.1016/j.crohns.2013.08.002

Kaser, A., S. Zeissig, and R.S. Blumberg. 2010. Inflammatory bowel disease. *Annu. Rev. Immunol.* 28:573–621. https://doi.org/10.1146/annurev-immunol-030409-101225

Khor, B., A. Gardet, and R.J. Xavier. 2011. Genetics and pathogenesis of inflammatory bowel disease. *Nature.* 474:307–317. https://doi.org/10.1038/nature10209

Kim, C., F. Ye, and M.H. Ginsberg. 2011. Regulation of integrin activation. *Annu. Rev. Cell Dev. Biol.* 27:321–345. https://doi.org/10.1146/annurev-cellbio-100109-104104

Klann, J.E., K.A. Remedios, S.H. Kim, P.J. Metz, J. Lopez, L.A. Mack, Y. Zheng, M.H. Ginsberg, B.G. Petrich, and J.T. Chang. 2017. Talin Plays a Critical Role in the Maintenance of the Regulatory T Cell Pool. *J. Immunol.* 198:4639–4651. https://doi.org/10.4049/jimmunol.1601165

Klann, J.E., S.H. Kim, K.A. Remedios, Z. He, P.J. Metz, J. Lopez, T. Tysl, J.G. Olvera, J.N. Ablack, J.M. Cantor, et al. 2018. Integrin Activation Controls Regulatory T Cell-Mediated Peripheral Tolerance. *J. Immunol.* 200:4012–4023. https://doi.org/10.4049/jimmunol.1800112

Klapproth, S., M. Sperandio, E.M. Pinheiro, M. Prünster, O. Soehnlein, F.B. Gertler, R. Fässler, and M. Moser. 2015. Loss of the Rap1 effector RIAM results in leukocyte adhesion deficiency due to impaired β2 integrin function in mice. *Blood.* 126:2704–2712. https://doi.org/10.1182/blood-2015-05-647453

Krause, M., J.D. Leslie, M. Stewart, E.M. Lafuente, F. Valderrama, R. Jagannathan, G.A. Strasser, D.A. Rubinson, H. Liu, M. Way, et al. 2004. Lamellipodin, an Ena/VASP ligand, is implicated in the regulation of lamellipodial dynamics. *Dev. Cell.* 7:571–583. https://doi.org/10.1016/j.devcel.2004.07.024

Kühn, R., J. Löhler, D. Rennick, K. Rajewsky, and W. Müller. 1993. Interleukin-10-deficient mice develop chronic enterocolitis. *Cell.* 75:263–274. https://doi.org/10.1016/0092-8674(93)80068-P

Lagarrigue, F., P. Vikas Anekal, H.S. Lee, A.I. Bachir, J.N. Ablack, A.F. Horwitz, and M.H. Ginsberg. 2015. A RIAM/lamellipodin-talin-integrin complex forms the tip of sticky fingers that guide cell migration. *Nat. Commun.* 6:8492. https://doi.org/10.1038/ncomms9492

Lagarrigue, F., F.B. Gertler, M.H. Ginsberg, and J.M. Cantor. 2017. Cutting Edge: Loss of T Cell RIAM Precludes Conjugate Formation with APC and Prevents Immune-Mediated Diabetes. *J. Immunol.* 198:3410–3415. https://doi.org/10.4049/jimmunol.1601743

Lahl, K., C. Loddenkemper, C. Drouin, J. Freyer, J. Arnason, G. Eberl, A. Hamann, H. Wagner, J. Huehn, and T. Sparwasser. 2007. Selective depletion of Foxp3+ regulatory T cells induces a scurfy-like disease. *J. Exp. Med.* 204:57–63. https://doi.org/10.1084/jem.20061852

Law, A.L., A. Vehlow, M. Kotini, L. Dodgson, D. Soong, E. Theveneau, C. Bodo, E. Taylor, C. Navarro, U. Perera, et al. 2013. Lamellipodin and the Scar/WAVE complex cooperate to promote cell migration in vivo. *J. Cell Biol.* 203:673–689. https://doi.org/10.1083/jcb.201304051

Lee, P.P., D.R. Fitzpatrick, C. Beard, H.K. Jessup, S. Lehar, K.W. Makar, M. Pérez-Melgosa, M.T. Sweetser, M.S. Schlissel, S. Nguyen, et al. 2001. A critical role for Dnmt1 and DNA methylation in T cell development, function, and survival. *Immunity.* 15:763–774. https://doi.org/10.1016/S1074-7613(01)00227-8

Lee, H.S., C.J. Lim, W. Puzon-McLaughlin, S.J. Shattil, and M.H. Ginsberg. 2009. RIAM activates integrins by linking talin to ras GTPase membrane-targeting sequences. *J. Biol. Chem.* 284:5119–5127. https://doi.org/10.1074/jbc.M807117200

Li, Y., J. Yan, P. De, H.C. Chang, A. Yamauchi, K.W. Christopherson II, N.C. Paranavitana, X. Peng, C. Kim, V. Munugalavadla, et al. 2007. Rap1a null mice have altered myeloid cell functions suggesting distinct roles for the closely related Rap1a and 1b proteins. *J. Immunol.* 179:8322–8331. https://doi.org/10.4049/jimmunol.179.12.8322

Li, Z., I. Arijs, G. De Hertogh, S. Vermeire, M. Noman, D. Bullens, L. Coorevits, X. Sagaert, F. Schuit, P. Rutgeerts, et al. 2010. Reciprocal changes of Foxp3 expression in blood and intestinal mucosa in IBD patients responding to infliximab. *Inflamm. Bowel Dis.* 16:1299–1310. https://doi.org/10.1002/ibd.21229

Maul, J., C. Loddenkemper, P. Mundt, E. Berg, T. Giese, A. Stallmach, M. Zeitz, and R. Duchmann. 2005. Peripheral and intestinal regulatory CD4+ CD25(high) T cells in inflammatory bowel disease. *Gastroenterology.* 128:1868–1878. https://doi.org/10.1053/j.gastro.2005.03.043

Neurath, M.F. 2014. Cytokines in inflammatory bowel disease. *Nat. Rev. Immunol.* 14:329–342. https://doi.org/10.1038/nri3661

Nourshargh, S., P.L. Hordijk, and M. Sixt. 2010. Breaching multiple barriers: leukocyte motility through venular walls and the interstitium. *Nat. Rev. Mol. Cell Biol.* 11:366–378. https://doi.org/10.1038/nrm2889

Ostanin, D.V., J. Bao, I. Koboziev, L. Gray, S.A. Robinson-Jackson, M. Kosloski-Davidson, V.H. Price, and M.B. Grisham. 2009. T cell transfer model of chronic colitis: concepts, considerations, and tricks of the trade. *Am. J. Physiol. Gastrointest. Liver Physiol.* 296:G135–G146. https://doi.org/10.1152/ajpgi.90462.2008

Petrich, B.G., P. Fogelstrand, A.W. Partridge, N. Yousefi, A.J. Ablooglu, S.J. Shattil, and M.H. Ginsberg. 2007a. The antithrombotic potential of selective blockade of talin-dependent integrin alpha IIb beta 3 (platelet GPIIb-IIIa) activation. *J. Clin. Invest.* 117:2250–2259. https://doi.org/10.1172/JCI31024

Petrich, B.G., P. Marchese, Z.M. Ruggeri, S. Spiess, R.A. Weichert, F. Ye, R. Tiedt, R.C. Skoda, S.J. Monkley, D.R. Critchley, and M.H. Ginsberg. 2007b. Talin is required for integrin-mediated platelet function in hemostasis and thrombosis. *J. Exp. Med.* 204:3103–3111. https://doi.org/10.1084/jem.20071800

Rice, G.P., H.P. Hartung, and P.A. Calabresi. 2005. Anti-alpha4 integrin therapy for multiple sclerosis: mechanisms and rationale. *Neurology.* 64:1336–1342. https://doi.org/10.1212/01.WNL.0000158329.30470.D0

Rubtsov, Y.P., J.P. Rasmussen, E.Y. Chi, J. Fontenot, L. Castelli, X. Ye, P. Treuting, L. Siewe, A. Roers, W.R. Henderson Jr., et al. 2008. Regulatory T cell–derived interleukin-10 limits inflammation at environmental interfaces. *Immunity.* 28:546–558. https://doi.org/10.1016/j.immuni.2008.02.017

Rutgeerts, P.J., R.N. Fedorak, D.W. Hommes, A. Sturm, D.C. Baumgart, B. Bressler, S. Schreiber, J.C. Mansfield, M. Williams, M. Tang, et al. 2013. A randomised phase I study of etrolizumab (rhuMAb β7) in moderate to severe ulcerative colitis. *Gut.* 62:1122–1130. https://doi.org/10.1136/gutjnl-2011-301769

Sandborn, W.J., B.G. Feagan, P. Rutgeerts, S. Hanauer, J.F. Colombel, B.E. Sands, M. Lukas, R.N. Fedorak, S. Lee, B. Bressler, et al. GEMINI 2 Study Group. 2013. Vedolizumab as induction and maintenance therapy for Crohn's disease. *N. Engl. J. Med.* 369:711–721. https://doi.org/10.1056/NEJMoa1215739

Shattil, S.J., C. Kim, and M.H. Ginsberg. 2010. The final steps of integrin activation: the end game. *Nat. Rev. Mol. Cell Biol.* 11:288–300. https://doi.org/10.1038/nrm2871

Smith, P.D., C. Ochsenbauer-Jambor, and L.E. Smythies. 2005. Intestinal macrophages: unique effector cells of the innate immune system. *Immunol. Rev.* 206:149–159. https://doi.org/10.1111/j.0105-2896.2005.00288.x

Song-Zhao, G.X., and K.J. Maloy. 2014. Experimental mouse models of T cell-dependent inflammatory bowel disease. *Methods Mol. Biol.* 1193:199–211. https://doi.org/10.1007/978-1-4939-1212-4_18

Stefanini, L., F. Ye, A.K. Snider, K. Sarabakhsh, R. Piatt, D.S. Paul, W. Bergmeier, and B.G. Petrich. 2014. A talin mutant that impairs talin-integrin binding in platelets decelerates αIIbβ3 activation without pathological bleeding. *Blood.* 123:2722–2731. https://doi.org/10.1182/blood-2013-12-543363

Stritt, S., K. Wolf, V. Lorenz, T. Vögtle, S. Gupta, M.R. Bösl, and B. Nieswandt. 2015. Rap1-GTP-interacting adaptor molecule (RIAM) is dispensable for platelet integrin activation and function in mice. *Blood.* 125:219–222. https://doi.org/10.1182/blood-2014-08-597542

Su, W., J. Wynne, E.M. Pinheiro, M. Strazza, A. Mor, E. Montenont, J. Berger, D.S. Paul, W. Bergmeier, F.B. Gertler, and M.R. Philips. 2015. Rap1 and its effector RIAM are required for lymphocyte trafficking. *Blood.* 126:2695–2703. https://doi.org/10.1182/blood-2015-05-644104

Sun, H., Y. Wu, J. Qi, Y. Pan, G. Ge, and J. Chen. 2011. The CC' and DE loops in Ig domains 1 and 2 of MAdCAM-1 play different roles in MAdCAM-1 binding to low- and high-affinity integrin alpha4beta7. *J. Biol. Chem.* 286:12086–12092. https://doi.org/10.1074/jbc.M110.208900

Sun, H., J. Liu, Y. Zheng, Y. Pan, K. Zhang, and J. Chen. 2014. Distinct chemokine signaling regulates integrin ligand specificity to dictate tissue-specific lymphocyte homing. *Dev. Cell.* 30:61–70. https://doi.org/10.1016/j.devcel.2014.05.002

Sun, H., F. Lagarrigue, A.R. Gingras, Z. Fan, K. Ley, and M.H. Ginsberg. 2018. Transmission of integrin β7 transmembrane domain topology enables gut lymphoid tissue development. *J. Cell Biol.* 217:1453–1465. https://doi.org/10.1083/jcb.201707055

Sun, H., W. Kuk, J. Rivera-Nieves, M.A. Lopez-Ramirez, L. Eckmann, and M.H. Ginsberg. 2020a. β7 Integrin Inhibition Can Increase Intestinal Inflammation by Impairing Homing of CD25hiFoxP3+ Regulatory T Cells. *Cell. Mol. Gastroenterol. Hepatol.* 9:369–385. https://doi.org/10.1016/j.jcmgh.2019.10.012

Sun, H., W. Kuk, J. Rivera-Nieves, M.A. Lopez-Ramirez, L. Eckmann, and M.H. Ginsberg. 2020b. β7 Integrin Inhibition Can Increase Intestinal Inflammation by Impairing Homing of CD25hiFoxP3+ Regulatory T Cells. *Cell. Mol. Gastroenterol. Hepatol.* 9:369–385. https://doi.org/10.1016/j.jcmgh.2019.10.012

Tran, D.Q., D.D. Glass, G. Uzel, D.A. Darnell, C. Spalding, S.M. Holland, and E.M. Shevach. 2009. Analysis of adhesion molecules, target cells, and role of IL-2 in human FOXP3+ regulatory T cell suppressor function. *J. Immunol.* 182:2929–2938. https://doi.org/10.4049/jimmunol.0803827

Villablanca, E.J., B. Cassani, U.H. von Andrian, and J.R. Mora. 2011. Blocking lymphocyte localization to the gastrointestinal mucosa as a therapeutic strategy for inflammatory bowel diseases. *Gastroenterology.* 140:1776–1784. https://doi.org/10.1053/j.gastro.2011.02.015

von Andrian, U.H., and B. Engelhardt. 2003. Alpha4 integrins as therapeutic targets in autoimmune disease. *N. Engl. J. Med.* 348:68–72. https://doi.org/10.1056/NEJMe020151

Watanabe, N., L. Bodin, M. Pandey, M. Krause, S. Coughlin, V.A. Boussiotis, M.H. Ginsberg, and S.J. Shattil. 2008. Mechanisms and consequences of agonist-induced talin recruitment to platelet integrin alphaIIbbeta3. *J. Cell Biol.* 181:1211–1222. https://doi.org/10.1083/jcb.200803094

Wong, E., T. Cohen, E. Romi, M. Levin, Y. Peleg, U. Arad, A. Yaron, M.E. Milla, and I. Sagi. 2016. Harnessing the natural inhibitory domain to control TNFα Converting Enzyme (TACE) activity in vivo. *Sci. Rep.* 6:35598. https://doi.org/10.1038/srep35598

Yamahashi, Y., P.J. Cavnar, L.E. Hind, E. Berthier, D.A. Bennin, D. Beebe, and A. Huttenlocher. 2015. Integrin associated proteins differentially regulate neutrophil polarity and directed migration in 2D and 3D. *Biomed. Microdevices.* 17:100. https://doi.org/10.1007/s10544-015-9998-x

Zhang, H., Y.C. Chang, M.L. Brennan, and J. Wu. 2014a. The structure of Rap1 in complex with RIAM reveals specificity determinants and recruitment mechanism. *J. Mol. Cell Biol.* 6:128–139. https://doi.org/10.1093/jmcb/mjt044

Zhang, J., S. Fu, S. Sun, Z. Li, and B. Guo. 2014b. Inflammasome activation has an important role in the development of spontaneous colitis. *Mucosal Immunol.* 7:1139–1150. https://doi.org/10.1038/mi.2014.1

Zhang, H.L., Y.J. Zheng, Y.D. Pan, C. Xie, H. Sun, Y.H. Zhang, M.Y. Yuan, B.L. Song, and J.F. Chen. 2016. Regulatory T-cell depletion in the gut caused by integrin β7 deficiency exacerbates DSS colitis by evoking aberrant innate immunity. *Mucosal Immunol.* 9:391–400. https://doi.org/10.1038/mi.2015.68
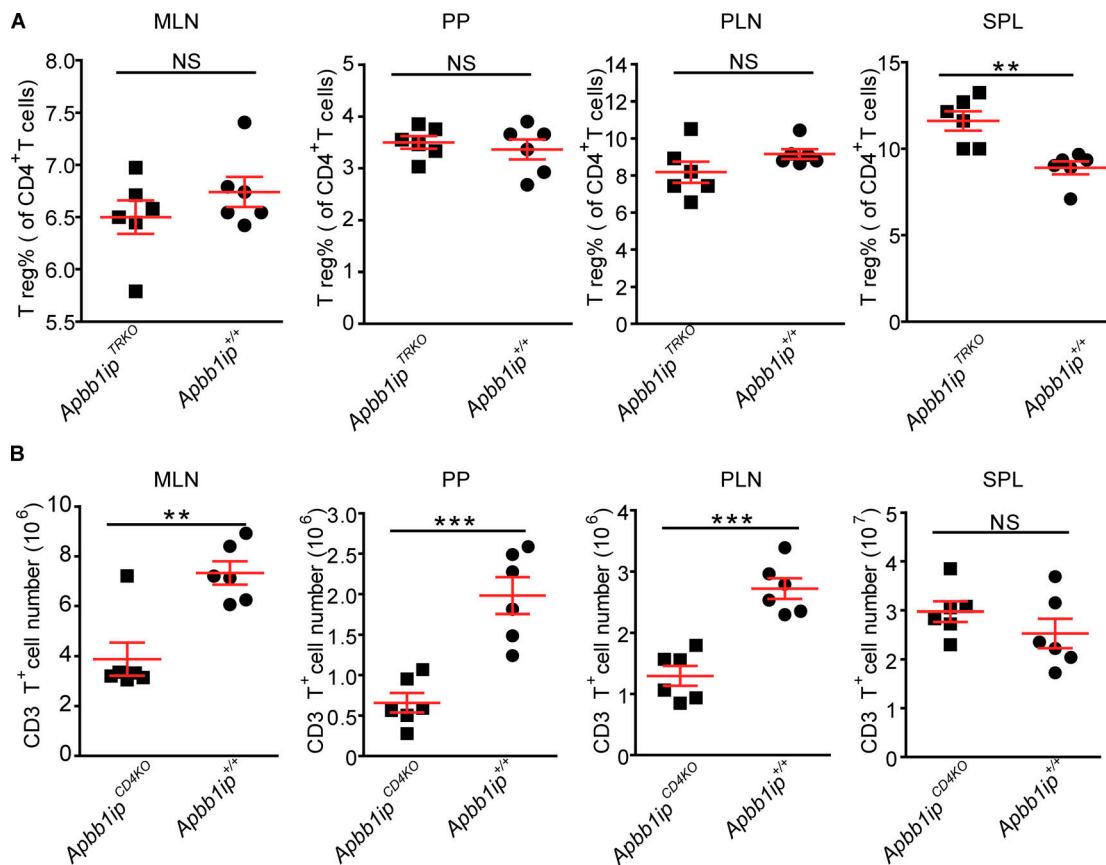
Figure S1. **Apbb1ip^TRKO mice show a similar number and percentage of T reg cells in lymphoid organs. (A and B)** The percentage of T reg cells in MLNs, PPs, PLNs, and SPs from *Apbb1ip^{+/+}* (*Apbb1ip^{wt/wt},Foxp3^{YFP-Cre}*) or *Apbb1ip^{TRKO}* mice ($n = 6$; A), and *Apbb1ip^{+/+}* (*Apbb1ip^{wt/wt},CD4^{Cre}*) or *Apbb1ip^{CD4KO}* mice ($n = 6$; B). $n = 3$ mice per group. Data are representative of two independent experiments. Data represent mean ± SEM. **, $P < 0.01$; ***, $P < 0.001$; two-tailed *t* test. *Apbb1ip^{+/+}*, *Apbb1ip^{wt/wt},Foxp3^{YFP-Cre}* mice or *Apbb1ip^{wt/wt},CD4^{Cre}* mice; *Apbb1ip^{TRKO}*, *Apbb1ip^{fl/fl},Foxp3^{YFP-Cre}* mice; CD4KO, CD4^+ T cell–specific knockout; SPL, spleen; *TRKO*, T reg cell–specific RIAM knockout.
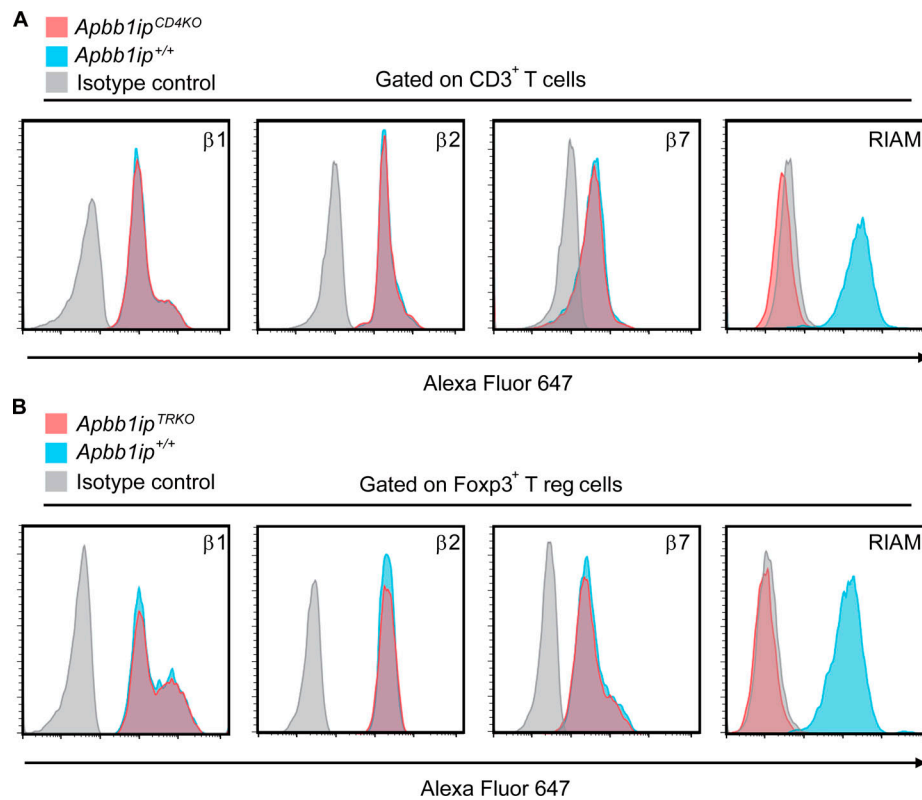
Figure S2.   **Integrin expression in RIAM-null T cells and T reg cells. (A and B)** Surface expression of integrin β1, β2, β7, and intracellular expression of RIAM in *Apbb1ip*$^{+/+}$ (*Apbb1ip*$^{wt/wt}$,*CD4*^{Cre}) or *Apbb1ip*^{CD4KO} (*Apbb1ip*$^{fl/fl}$,*CD4*^{Cre}) mice (A) and *Apbb1ip*$^{+/+}$ (*Apbb1ip*$^{wt/wt}$,*Foxp3*$^{YFP-Cre}$) or *Apbb1ip*^{TRKO} (*Apbb1ip*$^{fl/fl}$,*Foxp3*$^{YFP-Cre}$) mice (B). Representative histograms are displayed. Data are representative of three independent experiments. *Apbb1ip*$^{+/+}$, *Apbb1ip*$^{wt/wt}$,*Foxp3*$^{YFP-Cre}$ mice or *Apbb1ip*$^{wt/wt}$,*CD4*^{Cre} mice; *Apbb1ip*^{TRKO}, *Apbb1ip*$^{fl/fl}$,*Foxp3*$^{YFP-Cre}$ mice; CD4KO, CD4^{+} T cell–specific knockout; *TRKO*, T reg cell–specific RIAM inactivation.
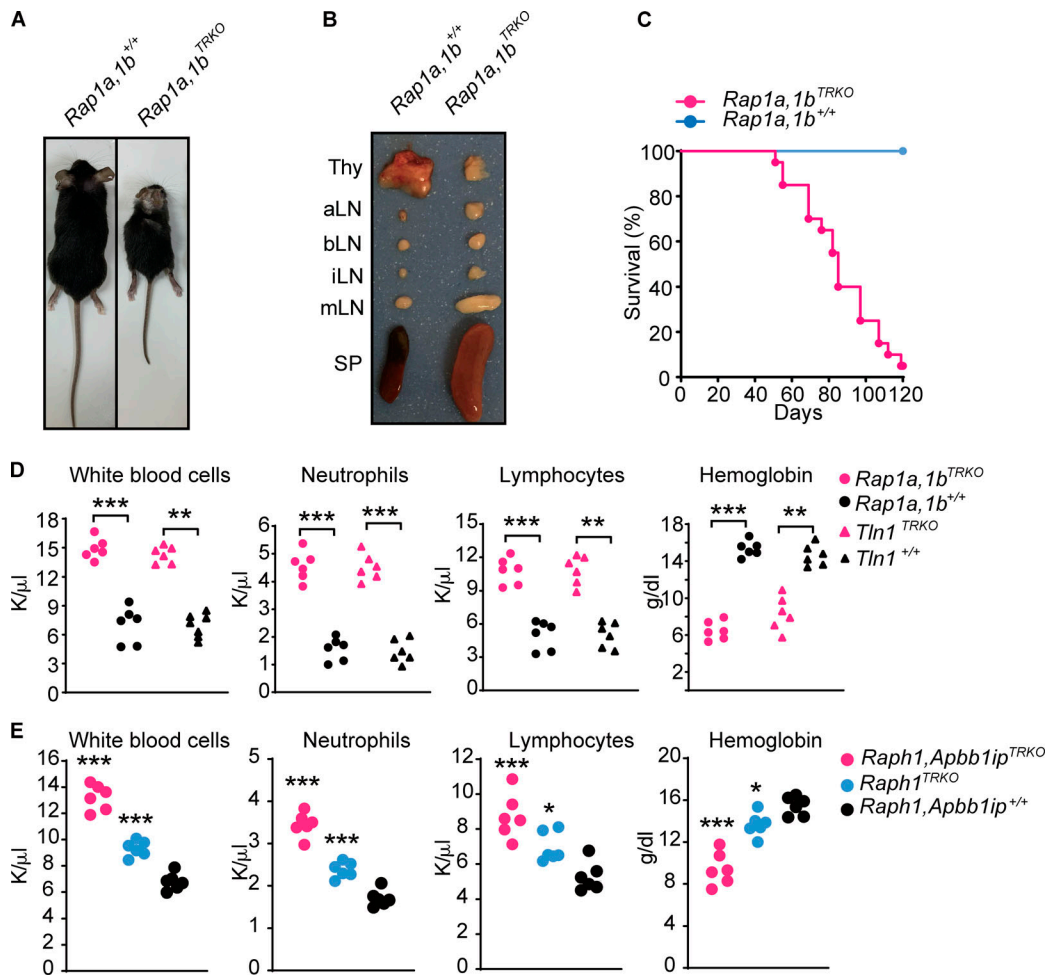
Figure S3. **Phenotype of *Rap1a,1b* ^{TRKO} mice, and complete blood counts of these T reg cell–specific gene–depleted mice. (A–C)** Representative morphology (A) and organs (SP, thymus [Thy], and LNs, including aortic LN [aLN], brachial LN [bLN], mLN, and inguinal LN [iLN]; B) from male *Rap1a,1b*$^{+/+}$ and *Rap1a,1b* ^{TRKO} mice. **(C)** Survival of *Rap1a,1b*$^{+/+}$ and *Rap1a,1b* ^{TRKO} mice. **(D and E)** Complete blood counts of *Rap1a,1b*$^{+/+}$, *Rap1a,1b* ^{TRKO}, *TLN1*$^{+/+}$, or *TLN1*^{TRKO} mice (D) and *Raph1,Apbb1ip*^{TRKO}, *Raph1*^{TRKO}, and *Raph1,Apbb1ip*$^{+/+}$ mice (E). *n* = 3 mice per group. Data are representative of two independent experiments. Data represent mean ± SEM. *, P < 0.05; **, P < 0.01; ***, P < 0.001; one-way ANOVA with Bonferroni posttest. *Rap1a,b*$^{+/+}$, *Rap1a*$^{wt/wt}$,*Rap1b*$^{wt/wt}$,*Foxp3*$^{YFP-Cre}$ mice; *Rap1a,b*^{TRKO}, *Rap1a*$^{fl/fl}$,*Rap1b*$^{fl/fl}$,*Foxp3*$^{YFP-Cre}$ mice; *TLN1*$^{+/+}$, *TLN1*$^{wt/wt}$,*Foxp3*$^{YFP-Cre}$ mice; *TLN1*^{TRKO}, *TLN1*$^{fl/fl}$,*Foxp3*$^{YFP-Cre}$ mice; *Raph1,Apbb1ip*$^{+/+}$, *Raph1*$^{wt/wt}$,*Apbb1ip*$^{wt/wt}$,*Foxp3*$^{YFP-Cre}$ mice; *Raph1*^{TRKO}, *Raph1*$^{fl/fl}$,*Foxp3*$^{YFP-Cre}$ mice; *Raph1,Apbb1ip*^{TRKO}, *Raph1*$^{fl/fl}$,*Apbb1ip*$^{fl/fl}$,*Foxp3*$^{YFP-Cre}$ mice; *TRKO*, T reg cell–specific RIAM knockout. K, 10^3.

Figure S4. **Lpd-deficient Tconv cells show normal integrin activation.** Binding of soluble ICAM-1, VCAM-1, or MAdCAM-1 to splenic T cells isolated from *Raph1,Apbb1ip*$^{+/+}$, *Raph1*^{CD4KO}, *Apbb1ip*^{CD4KO}, or *Raph1,Apbb1ip*^{CD4KO} mice in the presence or absence of PMA (100 nM). Data are representative of three independent experiments. Data represent mean ± SEM. ***, P < 0.001, one-way ANOVA with Bonferroni posttest.
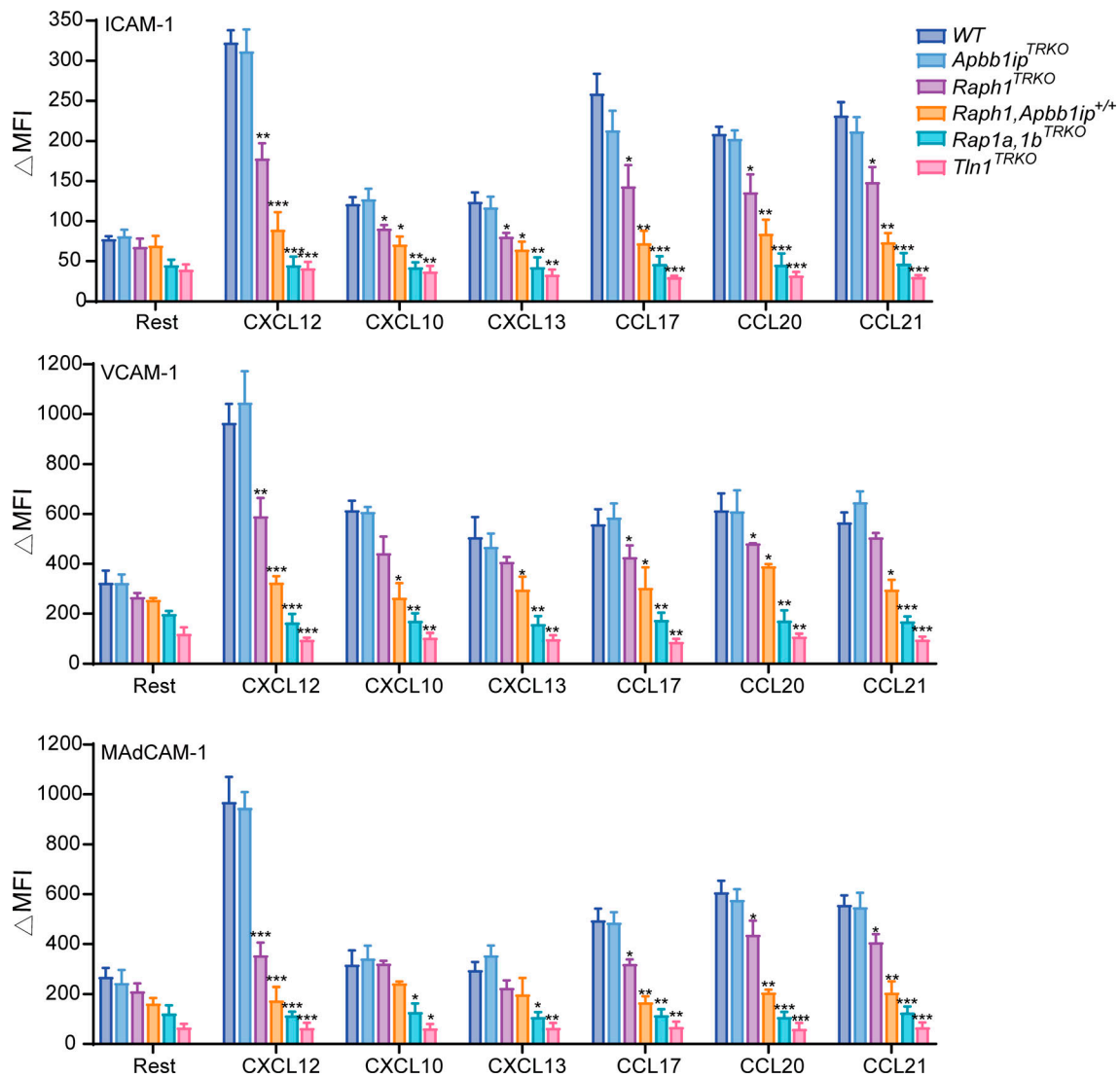
Figure S5.   **Chemokine-induced integrin activation in T reg cells.** Binding of soluble ICAM-1, VCAM-1, or MAdCAM-1 to YFP$^+$ T reg cells isolated from *WT*, *Apbb1ip^{TRKO}*, *Raph1^{TRKO}*, *Raph1,Apbb1ip^{TRKO}*, *Rap1a,1b ^{TRKO}*, *TLN1$^{+/+}$*, and *TLN1^{TRKO}* mice in the presence or absence of different chemokines (1 μM). Data are representative of five independent experiments. Data represent mean ± SEM. *, $P < 0.05$; **, $P < 0.01$; ***, $P < 0.001$; one-way ANOVA with Bonferroni posttest. MFI, mean fluorescence intensity; *Apbb1ip^{TRKO}*, *Apbb1ip$^{fl/fl}$,Foxp3$^{YFP-Cre}$* mice; *Raph1^{TRKO}*, *Raph1$^{fl/fl}$,Foxp3$^{YFP-Cre}$* mice; *Raph1,Apbb1ip^{TRKO}*, *Raph1$^{fl/fl}$,Apbb1ip$^{fl/fl}$,Foxp3$^{YFP-Cre}$* mice; *Rap1a,b^{TRKO}*, *Rap1a$^{fl/fl}$,Rap1b$^{fl/fl}$,Foxp3$^{YFP-Cre}$* mice; *TLN1^{TRKO}*, *TLN1$^{fl/fl}$,Foxp3$^{YFP-Cre}$* mice; *TRKO*, T reg cell–specific RIAM knockout; *WT*, *Foxp3$^{YFP-Cre}$* mice.